

**MINIMAL REFLECTION SURFACES IN  $\mathbb{S}^3$ .  
COMBINATORICS OF CURVATURE LINES AND MINIMAL SURFACES BASED ON  
FUNDAMENTAL PENTAGONS.**

ALEXANDER I. BOBENKO, SEBASTIAN HELLER, AND NICK SCHMITT

ABSTRACT. We study compact minimal surfaces in the 3-sphere which are constructed by successive reflections from a minimal  $n$ -gon — so-called minimal reflection surfaces. The minimal  $n$ -gon solves a free boundary problem in a fundamental piece of the respective reflection group. We investigate the combinatorics of the curvature lines of reflection surfaces, and construct new examples of minimal reflection surfaces based on pentagons. We end the paper by discussing the area of these minimal surfaces.

### Introduction

In 1978, Lawson [26] constructed a 2-integer family of embedded minimal surfaces  $\xi_{k,l}$  in the 3-sphere, by using the Plateau solutions for appropriate geodesic 4-gons. After only a few examples of compact minimal surfaces in the 3-sphere were known for a long time, new methods of construction have been developed in recent years. In particular, Kapouleas et al applied gluing methods for doubling Clifford tori and spheres [19, 20], the min-max theory of Marques and Neves [27] has been used to produce many equivariant minimal surfaces [24], and very recently work using Laplace and Steklov eigenvalues optimization in the presence of a discrete symmetry group has produced further examples [23]. Different methods often provide the same examples, but it is not trivial to distinguish between them even in specific cases [21]. In addition to these analytical methods, the more algebro-geometric integrable systems methods have also been used in recent years to study minimal surfaces and their properties, e.g. [16, 12, 15]. Besides detailed

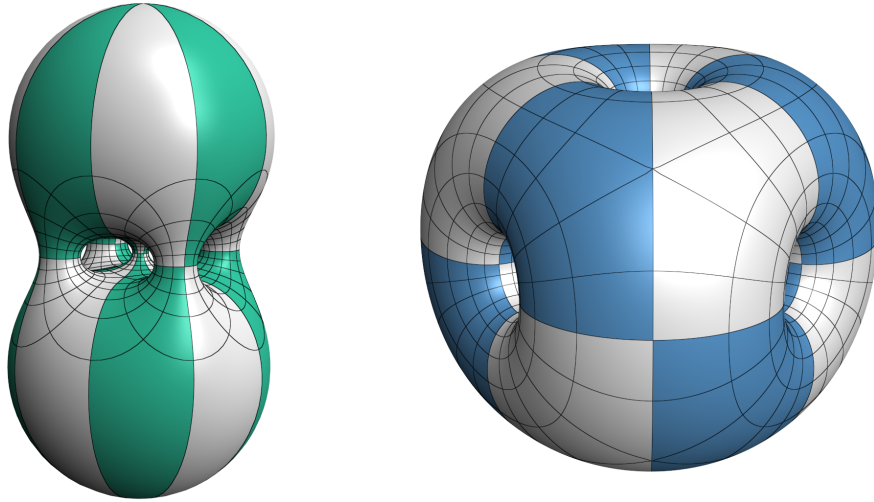


FIGURE 1. Two new minimal surfaces of genus 4.

experimental investigations such as in [1], these methods also provide the possibility of obtaining precise statements about geometric quantities like the area [15, 13].

The Lawson surfaces can also be constructed by first solving a free boundary problem for minimal surfaces contained in a certain tetrahedron, and then building up a closed surface through repetitive reflections across the geodesic faces of the tetrahedron. Of course, these tetrahedra must be fundamental pieces of a finite reflection group – namely  $D_m \times D_n$  in the case of the Lawson surfaces – in order to obtain a closed surface. This method has been first applied by Karcher-Pinkall-Sterling [22], when they constructed new minimal surfaces in  $\mathbb{S}^3$  built out of free boundary minimal surfaces in tetrahedrons which themselves are fundamental domains for (some of) the exceptional finite subgroups of  $O(4)$ , see Table 1 below. In both cases, the minimal surface  $S$  has a fundamental piece  $P$  which is a 4-gon, or, equivalently, there is a finite reflection group  $G$  with an order two subgroup  $\Gamma$  consisting of orientation preserving symmetries such that  $S \rightarrow S/\Gamma = \mathbb{CP}^1$  is branched over exactly 4 points.

In [1] we have studied minimal and constant mean curvature (CMC) surfaces in  $\mathbb{S}^3$  and  $\mathbb{R}^3$  which are based on such fundamental quadrilaterals. In particular, we constructed some minimal surfaces in  $\mathbb{S}^3$  of KPS-type which were missing in their original work [22], e.g., a surface of genus 29 and a new surface of genus 11 with octahedral symmetry. It became clear that one should also construct surfaces with  $n$ -gons as fundamental pieces for  $n \geq 5$  and that one has to develop tools to distinguish the different surfaces. (It should be mentioned that, apart from the round sphere, no compact minimal surfaces based on fundamental 3-gons are possible.) For example, some of the minimal surfaces based on fundamental pentagons are actually Lawson or KPS surfaces. Therefore, in the first part of the paper we study reflection surfaces (for details see Definition 1.3 below), together with the (combinatorial) properties of their curvature lines. It is shown in Theorem 1.15 that each compact reflection surface has closed curvature lines, and we develop tools to distinguish different surface classes, see e.g. Theorem 1.17. As a consequence, we obtain that most minimal reflection surfaces obtained from fundamental pentagons are neither the Lawson nor the KPS surfaces.

It is worth mentioning that the treatment of reflection surfaces based on the combinatorics of their curvature lines is similar to approaches in Discrete Differential Geometry (DDG). Curvature line parameterization is naturally used for structure preserving discretizations in DDG. In [4] it was shown how the geometry of discrete minimal surfaces in Euclidean space is determined by the combinatorics of their curvature lines. The approach is based on the construction of a polyhedron with prescribed combinatorics whose edges are tangent to a sphere (Koebe polyhedron). The latter is interpreted as a discrete Gauss map of the corresponding surface. A similar method was recently developed in [3] for the construction of discrete surfaces of constant mean curvature from orthogonal ring patterns in  $\mathbb{S}^2$ . The orthogonal ring patterns are also uniquely determined by their combinatorics and can be interpreted as discrete curvature lines.

In the second part of the paper, we numerically construct a 2-integer family of embedded minimal surfaces with the same reflection symmetry groups as those of  $\xi_{k,l}$  with a fundamental pentagon solving a free boundary problem, using the DPW construction [10]. After recalling the basics of integrable surface theory in the first part of Section 2, we shortly explain the setup for our experiments (Section 2.5). These are based on a flow on the space of so-called reflection potentials, which is by now well-understood mathematically in the case of 4-gons, see [12, 14]. In Section 3, we explain in detail how to show the existence of reflection potentials for  $n$ -gons for any  $n \geq 4$ , which can then serve as initial conditions of our numerical flow.

Based on our experiments we conjecture the following surfaces: for each reflection group and each combinatorial way to inscribe a pentagon into a fundamental region there exists a minimal reflection surfaces in  $\mathbb{S}^3$  with the given combinatorics.

Some of these surfaces have already been proved to exist previously: Kapouleas doubling spheres instantiate minimal reflection surfaces for the dihedral families  $B_{2,k}$  and  $B_{k,2}$  for  $k$  sufficiently large [19, 20].

All images show the reflection surfaces in  $\mathbb{S}^3$  after stereographic projection to  $\mathbb{R}^3$ . A stereographic projection might break a symmetry of a surface, see for example Figure 6. All figures show the curvature lines of the surfaces, i.e., horizontal and vertical trajectories of the holomorphic quadratic Hopf differentials.

### Acknowledgements

The first author is partially supported by the DFG Collaborative Research Center TRR 109 *Discretization in Geometry and Dynamics*. The second author thanks the TU Berlin and the DFG Collaborative Research Center TRR 109 *Discretization in Geometry and Dynamics* for excellent research conditions and financial support during research stays when parts of the work were carried out. The second author is partially supported by the Beijing NSF *International Scientists Project*. The third author is supported by the DFG Collaborative Research Center TRR 109 *Discretization in Geometry and Dynamics*.

### 1. Reflection surfaces and combinatorics of curvature lines

**1.1. Reflection groups of  $\mathbb{S}^3$ .** We consider finite subgroups  $G \subset \text{Iso}(\mathbb{S}^3)$  of the group of isometries of the 3-sphere generated by reflections across totally geodesic 2-spheres. These groups are called *reflection groups*. Reflection groups and generalisations thereof in any dimension have been investigated and classified by Coxeter [7]. We also refer to [9].

In Table 1 below, we list all reflection groups faithfully acting on  $\mathbb{S}^3$ . The rank of the group indicates the number of generating reflection spheres. The diagram shows their intersections, indicating a fundamental polyhedron (or  $r$ -hedra)  $R$  of the reflection group.

**Proposition 1.1.** *The reflection groups acting on  $\mathbb{S}^3$  are as follows:*

group	rank	order	diagram	group	rank	order	diagram
{1}	0	1		$\text{oct} \times \mathbb{Z}_2$	4	96	
$\mathbb{Z}_2$	1	2		$\text{ico} \times \mathbb{Z}_2$	4	240	
$D_n$	2	$2n$		5-cell	4	120	
$D_n \times \mathbb{Z}_2$	3	$4n$		demitesseract	4	192	
tet	3	24		16-cell	4	384	
oct	3	48		24-cell	4	1152	
ico	3	120		600-cell	4	14400	
$D_m \times D_n$	4	$4mn$					
$\text{tet} \times \mathbb{Z}_2$	4	48					

TABLE 1. The reflection groups acting on  $\mathbb{S}^3$ .

*Proof.* See [8]. □

Fundamental polyhedra  $R$  have dihedral angles  $\frac{\pi}{n}$  with some integer  $n$ 's. The mark  $n$  in the diagrams in Table 1 denotes the dihedral angle  $\frac{\pi}{n}$  at the corresponding edge. Unmarked edges in the above table have integer  $n = 2$ . The groups in the families  $\mathbb{Z}_2 = D_1$ ,  $D_n$ ,  $D_n \times \mathbb{Z}_2$  and  $D_m \times D_n$  are referred to as dihedral, and the remaining eleven groups as non-dihedral.

1.2. **Reflection Surfaces.** A *star umbilic* on a surface in  $\mathbb{S}^3$  is an isolated umbilic with curvature line foliations as shown:

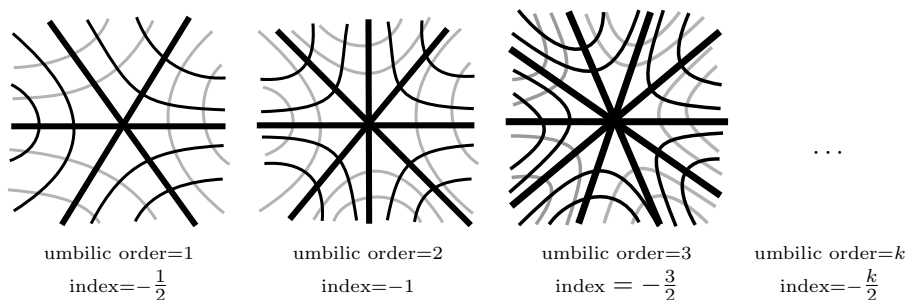


TABLE 2. Curvature line foliations at star umbilics.

An immersion  $f: M \rightarrow \mathbb{S}^3$  from an oriented surface  $M$  induces a Riemann surface structure on  $M$  such that  $f$  is conformal. Let  $K$  be the canonical bundle of the Riemann surface  $M$ . The Hopf differential of the surface  $f$  is the complex bilinear part of the second fundamental form, i.e.,

$$Q = II^{(2,0)} \in \Gamma(M, K^{\otimes 2}).$$

Therefore, the zeros of  $Q$  are exactly the umbilics of  $f$ . We assume that the zeros of  $Q$  are isolated. Then the index of a zero  $u$  of  $Q$  is defined as follows: consider a local holomorphic coordinate  $z$  centered at  $u$  and a smooth complex valued function  $q$  such that locally  $Q = q(dz)^2$ . Then the index of  $Q$  at  $u$  is the winding number of  $q/|q|: S^1 \cong \gamma \rightarrow S^1$ , where  $\gamma$  is a simple oriented loop around the isolated singularity  $u$ . If the index of a zero  $u$  of  $Q$  is positive, then  $u$  is a star umbilic. We define the *umbilic order*  $o_u$  of  $f$  at an umbilic  $u$  to be the index of the zero of  $Q$  at  $u$ .

**Remark 1.2.** The *index* of an star umbilic of umbilic order  $k$  is the winding number  $-k/2$  of the vector field tangent to a curvature line foliation along a small counterclockwise simple closed curve around the umbilic.

**Definition 1.3.** A *reflection surface* in  $\mathbb{S}^3$  is a smooth compact connected embedded orientable surface  $S \subset \mathbb{S}^3$  which is invariant under the action of a reflection group  $G$  acting on  $\mathbb{S}^3$  such that

- the fundamental region  $P \subset R$  of  $S$  inside a fundamental polyhedron  $R$  with respect to the action of  $G$  on  $\mathbb{S}^3$  is compact and simply connected;
- each umbilic on  $S$  is a star umbilic.

In particular, totally umbilical spheres are not reflection surfaces by the above definition. This allows us to exclude degenerate cases from further considerations. The examples of reflection

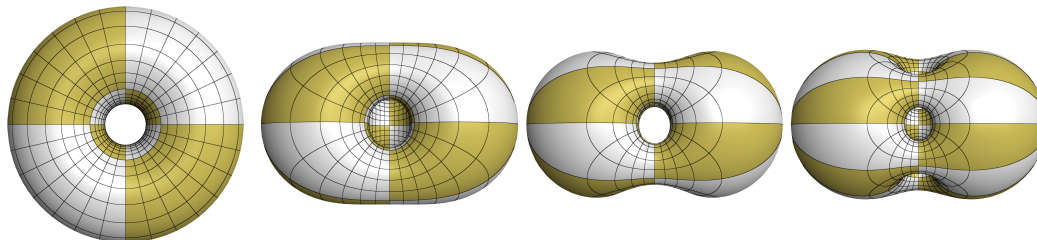


FIGURE 2. The dihedral family  $A_{1,n}$  for  $n = 2, \dots, 5$  (Lawson surfaces).

surfaces we are mainly interested in are given by minimal surfaces in the 3-sphere. These will be examined in detail in the next section.

The following proposition explains how a fundamental polygon of a reflection surface lies in a fundamental polyhedron.

**Proposition 1.4.** *Given a reflection surface  $S$  in  $\mathbb{S}^3$  with symmetry group  $G$ , let  $R$  be a fundamental polyhedron of the action of  $G$  on  $\mathbb{S}^3$ . Let  $P := S \cap R$  be a fundamental region of the action of  $G$  on  $S$ . Then  $P$  is an embedded topological disk with embedded boundary which is the union of curvature lines. Moreover,*

- (1) *The intersection of each face interior of  $R$  with  $S$  is a nonempty finite disjoint union of curves.*
- (2) *No two curves in a face of  $R$  share an endpoint.*
- (3) *The intersection of each edge interior of  $R$  with  $S$  is a finite set of points.*
- (4) *The intersection of each vertex of  $R$  with  $S$  is empty.*

*Proof.* The surface reflects in each face of the polyhedron. The surface cannot be contained in a face, because then it would be totally umbilic, contradicting that its umbilics are isolated. By the implicit function theorem, the surface intersects each face along a curve. Since the surface reflects in the faces, each such intersection curve is automatically a curvature line. To prove (1) it therefore remains to show that the intersection with each face is non-empty. In order to exclude non-empty intersection consider the totally geodesic 2-sphere containing the given face. The compact embedded and connected surface reflects across this 2-sphere. If the intersection of  $P$  with the face would be empty, the intersection of the compact surface with the 2-sphere would be empty as well, contradicting connectedness of  $S$ .

Since  $S$  is compact, (3) follows if we can show that  $S$  intersects each edge transversally. But transversality simply follows from the fact that the surface is embedded and has a well-defined tangential plane at every point.

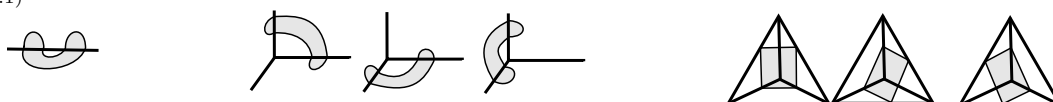
Likewise embeddedness of the surface implies (4), and it also shows that two boundary curves in the same face do not intersect (2). □

**1.3. Fundamental quadrilaterals and pentagons.** The following proposition lists the number of ways a  $p$ -gon can be placed in a marked fundamental  $r$ -hedra  $R$ , for  $p = 4, 5$  and  $r = 2, 3, 4$ . For  $p > 5$ , a corresponding list becomes more involved, while for  $p < 4$  there are no examples induced by reflection surfaces due to Corollary 1.11 below.

**Proposition 1.5.** *Let  $S$  be a reflection surface with fundamental  $r$ -hedra  $R$  and fundamental  $p$ -gon  $P$ , where  $r$  denotes the rank of the reflection group, see Table 1.*

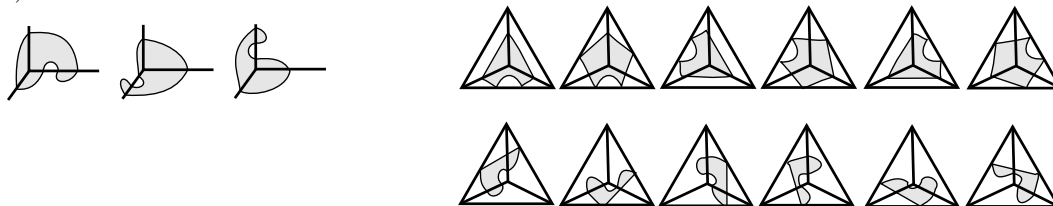
- (1) *For  $r = 2, 3, 4$ , there are respectively 1, 3, 3 ways a 4-gon (quadrilateral) can be placed in a marked  $r$ -hedra  $R$ , as shown:*

(1.1)



(2) For  $r = 2, 3, 4$ , there are 0, 3, 12 ways a 5-gon (pentagon) can be placed in a marked  $r$ -hedra  $R$ , as shown:

(1.2)



*Proof.* Number the  $r$  faces of the fundamental  $r$ -hedron  $R$  by  $1, \dots, r$ . Number each edge of the fundamental  $p$ -gon  $P$  with the number of the face of  $R$  in which it lies. Listing these integers cyclically, we obtain a cycle  $(n_1, \dots, n_p)$ . Two such cycles are considered to be the same up to the group generated by

- rotations  $(n_1, \dots, n_p) \mapsto (n_2, \dots, n_p, n_1)$ ,
- reversals  $(n_1, \dots, n_p) \mapsto (n_p, \dots, n_2, n_1)$ .

Moreover, the cycle satisfies

- no two consecutive integers in the cycle ( $(n_k, n_{k-1})$  or  $(n_p, n_1)$ ) are equal;
- each of the integers  $1, \dots, r$  appears at least once in the cycle (Proposition 1.4 (1)).

The number of ways to place  $P$  into the marked  $R$  is the number of these cycles. The number of ways to place  $P$  into the unmarked  $R$  is the number of these cycles modulo renumbering.

*4-gons.*

- If  $r \in \{0, 1\}$ , there are no cycles.
- If  $r = 2$ , the unique cycle is (1212).
- If  $r = 3$ , the unique cycle modulo renumbering is (1213), of which there are 3 permutations.
- If  $r = 4$ , the unique cycle modulo renumbering is (1234), of which there are 3 permutations.

*5-gons.*

- If  $r \in \{0, 1, 2\}$ , there are no cycles.
- If  $r = 3$ , the unique cycle modulo renumbering is (12123), of which there are 3 permutations.
- If  $r = 4$ , the unique cycle modulo renumbering is (12134), of which there are 12 permutations.  $\square$

Note that when edge integers (see Definition 1.6 below) are assigned to the fundamental polyhedron, renumbering of the faces gives rise to different reflection surfaces in general, e.g., the surfaces  $B_{k,\ell}$  and  $B_{\ell,k}$  are different for  $k \neq \ell$ , see for example the proof of Theorem 1.17 and Figure 7 and Figure 8 below.

**1.4. Genus.** The vertices and edges of a fundamental polygon of a reflection surface are assigned integers as follows.

**Definition 1.6.** Let  $S$  be a reflection surface with reflection group  $G$ , fundamental polyhedron  $R$ , and fundamental polygon  $P$ .

- Each vertex  $v$  of  $P$  lies on an edge  $e$  of  $R$ . The two edges  $e_1$  and  $e_2$  of  $P$  incident to  $v$  lie in two distinct faces  $f_1$  and  $f_2$  of  $R$ . Then  $f_1$  and  $f_2$  meet along  $e$  at an interior dihedral angle  $\pi/n$ ,  $n \in \mathbb{N}_{\geq 1}$ . Assign to  $v$  the *vertex integer*  $n$ .

- Each edge  $e$  of  $P$  lies in a face  $f$  of  $R$ . The two endpoints of  $e$  lie on two edges  $e_1$  and  $e_2$  of  $R$ . Let  $f_1$  and  $f_2$  be the faces of  $R$  such that  $f_1 \cap f = e_1$  and  $f_2 \cap f = e_2$ . Then  $f_1$  and  $f_2$  meet along an edge of  $R$  at an interior dihedral angle  $\pi/m$ ,  $m \in \mathbb{N}_{\geq 1}$ , and we assign to  $e$  the *edge integer*  $m$ .

The genus of a reflection surface  $S$  with finite reflection group  $G$  can be computed using that the tessellation of  $\mathbb{S}^3$  induced by  $G$  induces a tessellation of  $S$  into polygons.

**Theorem 1.7.** *Let  $S$  be a reflection surface with finite reflection group  $G$  of order  $|G| < \infty$ , and let  $P$  be a fundamental polygon with vertex integers  $(n_1, \dots, n_p)$  at its  $p \geq 4$  vertices. Then the genus of  $S$  is*

$$(1.3) \quad g = 1 + \frac{|G|}{4} \left( p - 2 - \sum_{k=1}^p \frac{1}{n_k} \right).$$

*Proof.* Let  $V, E, F$  be the number of vertices, edges and faces of  $S$ . Then

- the size of the orbit of vertex  $k$  of  $S$  is  $\frac{1}{2}|G|/n_k$ , so  $V = \frac{1}{2}|G| \sum_{k=1}^p \frac{1}{n_k}$ ;
- the size of the orbit of an edge of  $S$  is  $\frac{1}{2}|G|$ , so  $E = \frac{1}{2}|G|p$ ;
- $F = |G|$

As  $\chi = V - E + F$  is the Euler characteristic of  $S$ , and its genus satisfies  $g = 1 - \frac{1}{2}\chi$ , the result follows.  $\square$

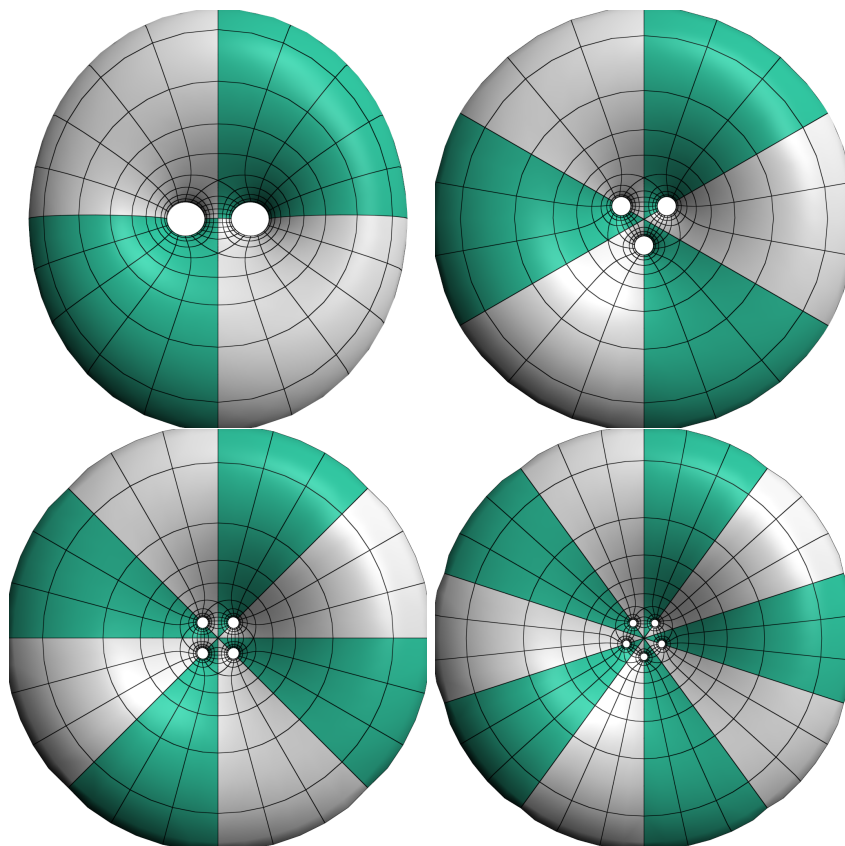


FIGURE 3. The dihedral family  $B_{n,1}$  for  $n = 2, \dots, 5$ .

**1.5. Curvature line polygons.** On a surface  $S$ , let  $V$  be the tangent vector field to a curvature line foliation, and let  $\gamma$  be a counterclockwise simple closed curve on  $S$  bounding a topological disk  $D$ . The *winding number* of  $V$  along  $\gamma$  is equal to the sum of the indices of the vector field at the umbilics in  $D$ .

**Definition 1.8.** A *curvature line polygon* on a surface is a  $p$ -gon bounding a topological disk whose edges are curvature lines, and all umbilics in  $P \cup \partial P$  are star umbilics.

The fundamental  $p$ -gon of a reflection surface is a curvature line polygon by Proposition 1.4.

**Definition 1.9.** The *umbilic excess* of a curvature line  $p$ -gon  $P$  is  $\kappa = \sum \kappa_u$ , where we sum over all umbilics  $u$  with umbilic order  $o_u$  of  $P$  and  $\kappa_u \in \frac{1}{2}\mathbb{N}_{\geq 0}$  is as follows:

$$\kappa_u = \begin{cases} \frac{(o_u+2-n_u)}{2n_u} & \text{if } u \text{ is a vertex umbilic;} \\ \frac{1}{2}o_u & \text{if } u \text{ is an edge umbilic;} \\ o_u & \text{if } u \text{ is a face umbilic.} \end{cases}$$

The following table shows some basic examples for the umbilic excess for umbilics lying on vertices, edges and faces of the  $p$ -gon  $P$ .

vertex umbilic				...
edge umbilic				...
face umbilic				...

TABLE 3. The umbilic excess for an umbilic  $u$  at a vertex, edge, or face of a polygon.

The following theorem generalizes the formula for the degree of the square of the canonical bundle of a reflection surface to a curvature line  $p$ -gon.

**Theorem 1.10.** *Let  $P$  be a curvature line  $p$ -gon (Definition 1.8) with umbilic excess  $\kappa$ . Then*

$$(1.4) \quad \kappa = \frac{1}{2}(p - 4) .$$

*Proof.* Draw a curvilinear polygon  $\gamma \subset P \cup \partial P$  with curvature line edges meeting at angles of  $\pm\pi/2$ , as shown in the following example:

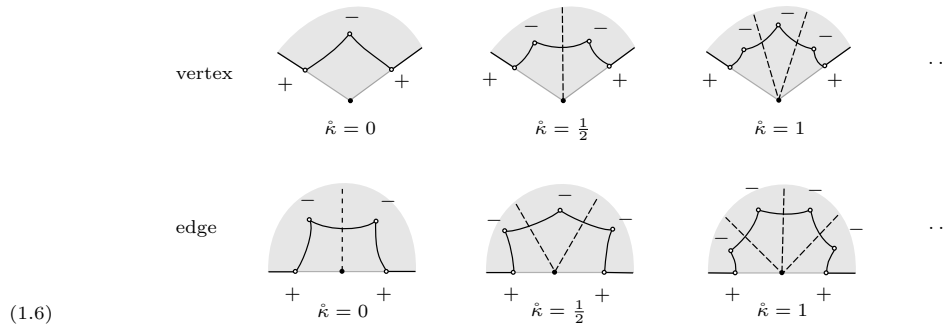




where

- near each vertex of  $P$ ,  $\gamma$  is as shown in the first row of (1.6);
- near each edge umbilic of  $P$ ,  $\gamma$  is as shown in the second row of (1.6);

and  $\hat{\kappa}$  denotes the umbilic excess of the respective umbilic.



Going along  $\gamma$  counterclockwise, let

- $\alpha$ : the sum of the turning angles at the vertices of  $\gamma$ ; each angle is  $\pm\pi/2$ ;
- $\beta$ : the sum of the turning angles of the edges of  $\gamma$ .

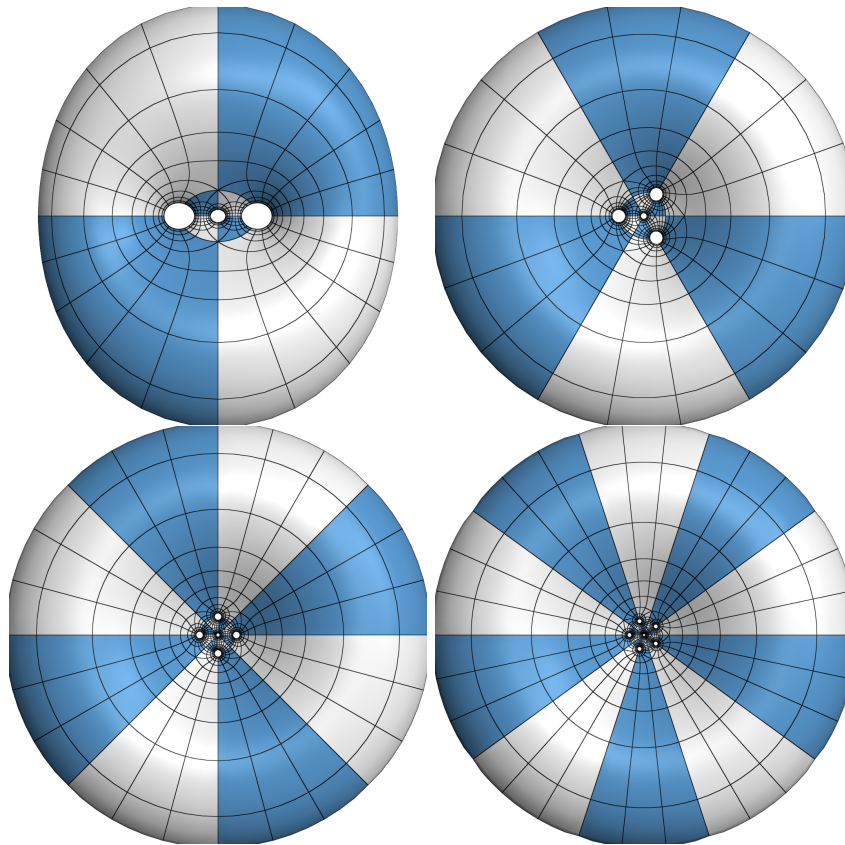


FIGURE 4. The dihedral family  $B_{2,n}$  for  $n = 2, \dots, 5$ .

Let  $\kappa_0$ ,  $\kappa_1$  and  $\kappa_2$  be the contributions to the umbilic excess  $\kappa$  of  $P$  at the vertex, edge and face umbilics respectively, so  $\kappa = \kappa_0 + \kappa_1 + \kappa_2$ .

Since  $\gamma$  is a simple closed curve,

$$(1.7) \quad \alpha + \beta = 2\pi .$$

Each vertex of  $P$  with umbilic excess  $\mathring{\kappa}$  contributes  $\pi(\frac{1}{2} - \mathring{\kappa})$  to  $\alpha$  (see the first row of (1.6)), so the  $p$  vertices of  $P$  contribute  $\pi(\frac{p}{2} - \kappa_0)$  to  $\alpha$ .

Each edge umbilic of  $P$  with umbilic excess  $\mathring{\kappa}$  contributes  $-\pi\mathring{\kappa}$  to  $\alpha$  (see the second row of (1.6)), so the edge umbilics of  $P$  contribute in total  $-\pi\kappa_1$  to  $\alpha$ .

Hence

$$(1.8) \quad \alpha = \pi(\frac{p}{2} - \kappa_0 - \kappa_1) .$$

Since  $\gamma$  encloses the face umbilics, then

$$(1.9) \quad \beta = -\pi\kappa_2 ,$$

see Remark 1.2. The result follows from (1.7), (1.8) and (1.9),  $\square$

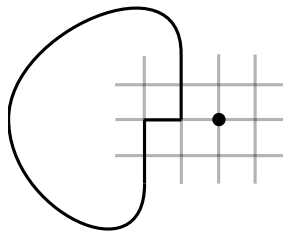
**Corollary 1.11.** *If  $P$  is a curvature line  $p$ -gon (Definition 1.8), then  $p \geq 4$ .*

*Proof.* This follows from Theorem 1.10 and the fact that  $\kappa \geq 0$ .  $\square$

**Theorem 1.12.** *Let  $D$  be a compact topological disk with boundary on which every umbilic is a star umbilic. Then every curvature line starting at a point  $p$  in the interior  $D$ , extended in either direction, either (a) ends at an umbilic in  $D$ , or (b) exits through the boundary of  $D$ .*

*Proof.* Let  $\gamma$  be a curvature line starting at  $p$ , extended in one direction, which does not end at an umbilic in  $D$ . If  $\gamma$  does not exit through the boundary of  $D$ , then  $\gamma$  has a limit point  $L$  in  $D$  because  $D$  is compact.

In the case  $L$  is in the interior of  $D$  and is not an umbilic, then near  $L$  the curvature lines make a checkerboard pattern: the gray lines in (1.10). Therefore there exists a 2-gon, one of whose edges is a segment of  $\gamma$ , the other a crossing curvature line, which bounds a disk as shown:



(1.10)

This contradicts Corollary 1.11.

The proofs for other cases ( $L$  is in the interior of  $D$  and is a star umbilic, or  $L$  is on the boundary of  $D$  and is either a non-umbilic or is a star umbilic) are similar.  $\square$

## 1.6. Foliations.

**Theorem 1.13.** *The curvature line foliations of quadrilaterals or pentagons bounded by curvature lines with star umbilics are as shown:*

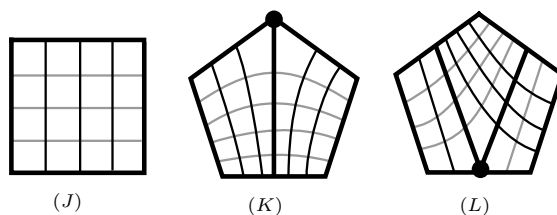


TABLE 4. (J): foliation of 4-gon by curvature lines. (K): foliation of a 5-gon by curvature lines, with the extra umbilic at a vertex. (L): foliation of a 5-gon by curvature lines, with the extra umbilic on an edge.

*Proof.* Let horizontal and vertical curvature lines be called  $\alpha$  and  $\beta$  respectively. If two curvature lines meet at a non-umbilic, then one is of type  $\alpha$  and the other of type  $\beta$ .

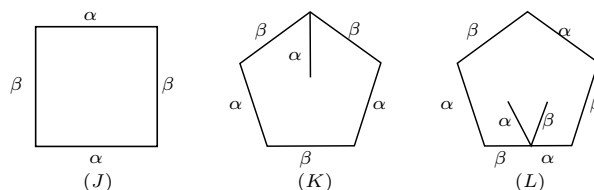


TABLE 5. Curvature lines on quadrilaterals and pentagons, in the two curvature line foliations  $\alpha$  and  $\beta$ .

*Quadrilaterals.* Let  $P$  be a quadrilateral bounded by curvature lines. By Theorem 1.10, the umbilic excess is  $\kappa = 0$ . Hence

- there are no curvature lines in the interior of  $P$  starting at a vertex,
- there are no umbilics on the edges of  $P$ , and
- there are no umbilics in the interior of  $P$ .

Hence the edges of  $P$  are cyclically of type  $\alpha, \beta, \alpha, \beta$ , as shown in Table 5(J).

Let  $\gamma$  be a curvature line of type  $\alpha$  through a point in the interior of  $P$ . Then  $\gamma$  does not end at a vertex of  $P$ , so by Theorem 1.12,  $\gamma$  starts and ends at edges of type  $\beta$ . By Corollary 1.11,  $\gamma$  cannot connect an edge to itself; otherwise there is a 2-gon bounding a disk. Hence  $\gamma$  connects opposite edges of  $P$  in a “checkerboard” pattern as in Table 4(J).

*Pentagons.* Let  $P$  be a quadrilateral bounded by curvature lines. By Theorem 1.10, the umbilic excess is  $\kappa = 1/2$ . Hence

- there are no umbilics in the interior of  $P$ ,
- either there is one vertex  $v$  of  $P$  from which one curvature line emanates into the interior  $P$ , as in Table 4(K), or
- there is a simple umbilic on an edge of  $P$ , as in Table 4(L).

Note that two intersecting curvature lines  $\gamma_1$  and  $\gamma_2$  have opposite types (if the point of intersection is not an umbilic): one is of type  $\alpha$  and the other of type  $\beta$ . Hence  $\gamma_1$  and  $\gamma_2$  exit the pentagon through edges of type  $\beta$  and  $\alpha$  respectively.

In case  $K$ , let  $\gamma$  be the curvature line through the vertex  $v$  of  $P$  into the interior of  $P$ , marked as type  $\alpha$ , where the edges of the pentagon are marked as shown in Table 5(K).

By Theorem 1.12,  $\gamma$  ends at a boundary edge of  $P$ . Since  $\gamma$  is of type  $\alpha$ , this edge is of type  $\beta$ . Since 2-gons bounding a disk are excluded by Corollary 1.11,  $\gamma$  ends at the edge of  $P$  opposite to  $v$ . This divides  $P$  into two quadrilaterals, each of which has a checkerboard curvature line pattern as shown in Table 4(K).

In case  $L$ , let  $\gamma_1$  and  $\gamma_2$  be the two curvature lines emanating from the edge umbilic into the interior of  $P$ , marked as  $\alpha$  and  $\beta$  respectively, as shown in Table 5(L).

It follows that  $\gamma_1$  and  $\gamma_2$  are as in Table 4(L); otherwise  $\gamma_1$  and  $\gamma_2$  would intersect, bounding a 2-gon, in contradiction to Corollary 1.11. This divides  $P$  into three quadrilaterals, each of which has a checkerboard curvature line pattern as shown in Table 4(L).  $\square$

**1.7. Quadrilateral decomposition and closed curvature lines.** A *curvature line quadrilateral decomposition* of a surface  $S$  is a cell decomposition of  $S$  such that each face is a quadrilateral, each edge is a curvature line and each vertex has an even number of edges emanating from it.

**Theorem 1.14.** *Every reflection surface has a curvature line quadrilateral decomposition.*

*Proof.* Let  $P$  be a fundamental polygon. In  $P$ , draw every curvature line starting at an umbilic. This decomposes  $P$  into finitely many curvature line quadrilaterals (see Definition 1.8).

Indeed, each sub-polygon satisfies: (a)  $P$  has no umbilics in its interior or on its edges, and (b) no curvature line in the interior of  $P$  ends at a vertex of  $P$ . Hence the umbilic excess of each sub-polygon is 0. By Theorem 1.10, each sub-polygon is a quadrilateral.  $\square$

A reflection surface has *closed curvature lines* if

- every curvature line which starts at an umbilic ends at an umbilic.
- every curvature line which does not pass through an umbilic is closed.

**Theorem 1.15.** *Let  $S$  be a reflection surface in  $\mathbb{S}^3$ . Then  $S$  has closed curvature lines.*

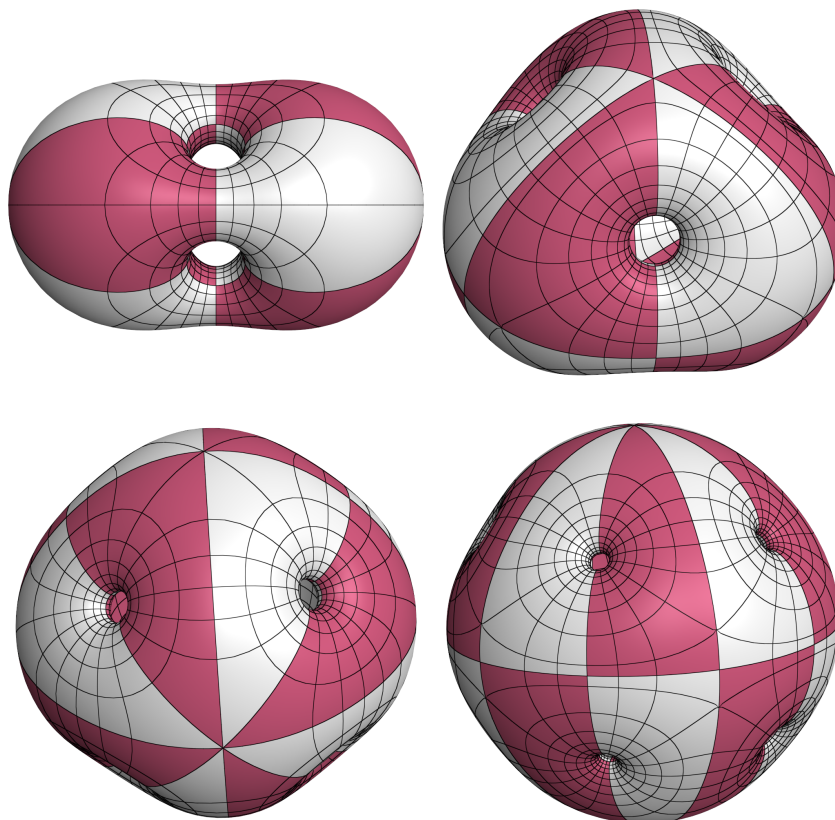


FIGURE 5. The dihedral family  $B_{n,2}$  for  $n = 2, \dots, 5$ .

*Proof.* Let  $R$  be a fundamental polyhedron and  $P$  be a fundamental polygon. In  $\mathbb{S}^3$ , every two faces of  $R$  meet at internal dihedral angle  $\pi/n$  for some  $n \in \mathbb{N}_{\geq 2}$ .

Let  $\gamma$  be a curvature line in  $P \cup \partial P$ .

Case 1:  $\gamma$  does not contain any umbilics. By Theorem 1.12,  $\gamma$  connects two edges  $e_1$  and  $e_2$  of  $P$ , meeting them perpendicularly. Let  $f_1$  and  $f_2$  be the two faces of the fundamental polyhedron containing  $e_1$  and  $e_2$  respectively.

Let  $H$  be the dihedral group generated by reflections in  $f_1$  and  $f_2$ , and let  $\delta$  be the orbit of  $\gamma$  under this group action. Then  $\delta$  is a smooth closed curvature line.

Case 2:  $\gamma$  connects an umbilic to an edge  $e$ . Since the surface reflects in the edge  $e$ ,  $\gamma$  reflects in the edge smoothly to  $\gamma'$ . The union  $\gamma \cup \gamma'$  is a smooth curvature line connecting two umbilics.

Case 3:  $\gamma$  connects two umbilics. In this case, we are done.

Case 4:  $\gamma$  is an edge  $e$  of  $P$ . Let  $v_1$  and  $v_2$  be the endpoints of  $e$ , i.e. vertices of  $P$ . The proof is as above in the three different cases, according to whether  $e_1$  and  $e_2$  are umbilics.  $\square$

**1.8. Two dihedral families of reflection surfaces.** Define the two 2-integer families of reflection surface types

$$(1.11) \quad A_{k,\ell} \quad (k, \ell) \in \mathbb{N}_{\geq 2} \times \mathbb{N}_{\geq 2} \quad \text{and} \quad B_{k,\ell} \quad (k, \ell) \in \mathbb{N}_{\geq 2} \times \mathbb{N}_{\geq 1}$$

with dihedral symmetry and respective fundamental quadrilateral and pentagon, as shown in Table 6:

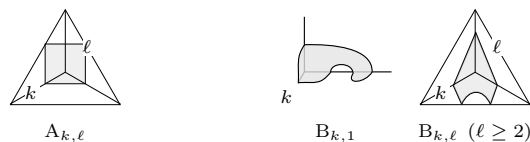


TABLE 6. Two 2-integer families  $A_{k,\ell}$  and  $B_{k,\ell}$  with dihedral symmetry and fundamental quadrilateral and pentagon respectively.

Then:

- $A_{k,\ell}$  is symmetric in  $k$  and  $\ell$ , while  $B_{k,\ell}$  is not.
- $\text{genus}(A_{k,\ell}) = (k-1)(\ell-1)$  and  $\text{genus}(B_{k,\ell}) = (k-1)(\ell-1) + k$ .
- The symmetry group of a reflection surface of type  $A_{k,\ell}$  is  $D_k \times D_\ell$ , see Theorem 1.16 below.
- The symmetry group of a reflection surface of type  $B_{k,\ell}$  has as subgroup  $D_k \times D_\ell$ .
- The Lawson surface  $\xi_{k-1,\ell-1}$  is a reflection surface of type  $A_{k,\ell}$ .

**Theorem 1.16.** *The reflection group of a surface of type  $A_{k,\ell}$ ,  $(k, \ell) \neq (2, 2)$  is exactly  $D_k \times D_\ell$ .*

*Proof.* If the surface had a larger symmetry group, its fundamental quadrilateral would be tessellated into quadrilateral as in Table 4(J).

The vertex integers around the fundamental quadrilateral, in cyclic order, are  $k, 2, \ell, 2$ . Since these reflect, they introduce umbilic on the vertices, edges or interior of the quadrilateral, which is impossible.  $\square$

The *umbilic structure* of a reflection surface  $S$  counts how many umbilics it has of what orders, written (non-uniquely) as a finite formal sum

$$(1.12) \quad \mathcal{U}(S) := n_1[o_1] + \cdots + n_s[o_s]$$

Since the genus  $g$  of  $S$  is related to the umbilic structure by

$$(1.13) \quad 4g - 4 = \sum_{k=1}^s n_k o_k \quad ,$$

two surfaces with the same umbilic structure have the same genus.

**Theorem 1.17.** *Every reflection surface of type*

$$(1.14) \quad \{B_{k,\ell} \mid (k, \ell) \notin \{(2, 1), (2, 2)\}\}$$

*is different from every reflection surface of type  $A_{u,v}$ .*

*Proof.* The umbilic structures of a reflection surface  $S$  of type  $A_{u,v}$  is

$$(1.15) \quad \mathcal{U}(A_{u,v}) = 2v[u - 2] + 2u[v - 2] .$$

A surface of type  $B_{k,\ell}$  may have different umbilic structures depending on the position of the extra umbilic, denoted as follows:

- $B_{k,\ell}^\alpha$  with extra umbilic on an edge of the pentagon,
- $B_{k,\ell}^\beta$  with extra umbilic at a vertex of the pentagon with vertex integer 2,
- $B_{k,\ell}^\gamma$ ,  $k > 2$  with extra umbilic at the vertex of the pentagon with vertex integer  $k$ .

The umbilic structures of the reflection surfaces of type  $B_{k,\ell}^x$ ,  $x \in \{\alpha, \beta, \gamma\}$  are:

$$(1.16) \quad \mathcal{U}(B_{k,\ell}^\alpha) = 2k\ell[1] + 2\ell[k - 2] , \quad \mathcal{U}(B_{k,\ell}^\beta) = k\ell[2] + 2\ell[k - 2] , \quad \mathcal{U}(B_{k,\ell}^\gamma) = 2\ell[2k - 2] .$$

Comparing the umbilic structures (1.15) with (1.16), the reflection surfaces of type  $A_{k,\ell}$  and those of type  $B_{u,v}$  with the same umbilic structure are:

$$(1.17) \quad \begin{array}{l|l} \text{(a)} \quad \mathcal{U}(A_{2,3}) = \mathcal{U}(B_{2,1}^\alpha) = 4[1] & \text{(d)} \quad \mathcal{U}(A_{4,4}) = \mathcal{U}(B_{2,8}^\beta) = 16[2] \\ \text{(b)} \quad \mathcal{U}(A_{2,4}) = \mathcal{U}(B_{2,2}^\beta) = 4[2] & \text{(e)} \quad \mathcal{U}(A_{2k,2k}) = \mathcal{U}(B_{k,4k}^\gamma) = 8k[2k - 2] \\ \text{(c)} \quad \mathcal{U}(A_{3,3}) = \mathcal{U}(B_{2,3}^\alpha) = 12[1] & \text{(f)} \quad \mathcal{U}(A_{2k,2}) = \mathcal{U}(B_{k,2}^\gamma) = 4[2k - 2] \end{array}$$

By Theorem 1.16 the symmetry group of reflection surfaces of type  $A_{u,v}$ ,  $(u, v) \neq (2, 2)$  is  $D_u \times D_v$ . Hence if a reflection surface of type  $B_{k,\ell}$  is of type  $A_{u,v}$ , then  $D_k \times D_\ell$  is a subgroup of  $D_u \times D_v$ , that is  $(k|u$  and  $\ell|v)$  or  $(k|v$  and  $\ell|u)$ . This excludes the pairs (1.17)(c), (d) and (e); that is for these pairs, the  $B$  surface is different from the corresponding  $A$  surface the same umbilic structure.

To show the pairs (1.17)(f) are different, assume  $A_{2k,2}$  and  $B_{k,2}^\gamma$  are the same. Since the extra umbilic of  $B_{k,2}^\gamma$  is at the vertex marked  $k$ , by the curvature line foliation Theorem 1.13(K), there is a curvature line in the pentagon from this vertex to the opposite side of the pentagon, and the surface reflects in this curvature line. On the other hand, the vertex and edge integers (Definition 1.6), of the fundamental pentagon are as shown:

$$(1.18) \quad \begin{array}{c} \begin{array}{c} 2 \\ \diagdown \quad \diagup \\ 2 \quad k \\ \diagup \quad \diagdown \\ k \quad 2 \\ \diagdown \quad \diagup \\ 2 \quad 1 \quad 2 \\ \diagup \quad \diagdown \\ 2 \end{array} \end{array}$$

The edge integers do not reflect across the dotted curvature line, contradicting that  $A_{2k,2}$  and  $B_{k,2}^\gamma$  are the same.  $\square$

By Theorem 1.17, a minimal surface of type  $B_{k,\ell}$  in  $\mathbb{S}^3$  is not a Lawson surface  $\xi_{ab}$ . The Lawson surface  $\xi_{2,1}$  (see Figure 2) is actually a minimal surface of type  $B_{2,1}$ , see Figure 3, and the Lawson surface  $\xi_{3,1}$  is a minimal surface of type  $B_{2,2}^\beta$ , see Figure 5.

## 2. Minimal surfaces in $\mathbb{S}^3$ via DPW method

In this section we recall the basic principles of the DPW approach [10] to minimal surfaces in  $\mathbb{S}^3$ , based on their associated families of flat connections [17]. For details see [1, 15] and references therein.

**2.1. Minimal surfaces in  $\mathbb{S}^3$ .** A minimal surface  $f: \Sigma \rightarrow \mathbb{S}^3$  is a critical point of the area functional. As such, it is characterized by vanishing mean curvature  $H = 0$ . Because  $f$  is an immersion (by assumption)  $f$  induces a Riemannian metric and a conformal structure on  $\Sigma$ . We assume that  $\Sigma$  is orientable. This is particularly the case when  $\Sigma$  is compact and  $f$  is an embedding. Then  $\Sigma$  is equipped with the structure of a Riemann surface such that  $f$  is conformal. It is well-known that a conformal map from a Riemann surface to  $\mathbb{S}^3$  (or any other Riemannian manifold) is harmonic if and only if it is minimal. In fact, the tension and the mean curvature of  $f$  are related by

$$d^\nabla * df = 2HNdA$$

where  $\nabla$  is the pull-back of the Levi-Civita connection of  $\mathbb{S}^3$ ,  $H$ ,  $N$  and  $dA$  are the mean curvature, the normal and the induced area form of  $f$ , respectively.

A surface  $f$  in  $\mathbb{S}^3$  is uniquely determined by its first and its second fundamental forms up to spherical isometry. Conversely, every pair consisting of a Riemannian metric  $g$  and a symmetric bilinear form  $II$  satisfying the (spherical) Gauss-Codazzi equations is induced by an immersion

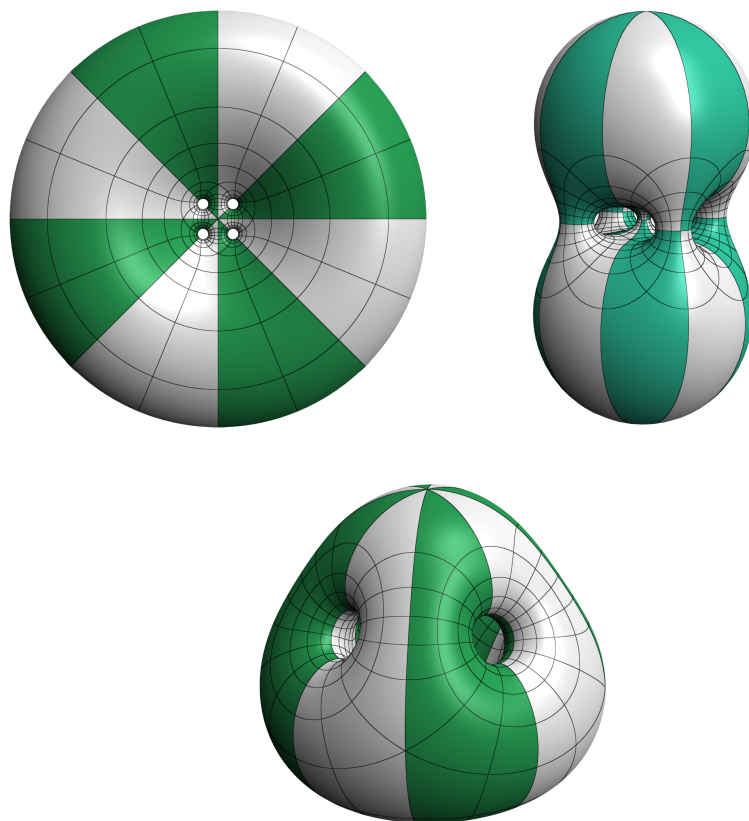


FIGURE 6. Three views (stereographic projections) of surface  $B_{4,1}$  of genus 4.

which, in general, is only well-defined on some covering. If  $f$  is conformal and minimal, then the second fundamental form

$$II = Q + \bar{Q}$$

is uniquely determined by a (complex) quadratic differential which turns out to be holomorphic

$$Q \in H^0(\Sigma, K_\Sigma^2).$$

In particular, every umbilic of  $f$  is a star umbilic. Rotating  $Q$  by some unimodular complex number  $\lambda \in \mathbb{S}^1$  yields a new solution

$$(g, \widetilde{II} = \lambda Q + \bar{\lambda} \bar{Q})$$

of the Gauss-Codazzi equations. Consequently, we obtain a  $\mathbb{S}^1$ -family of minimal surfaces  $f_\lambda$ , which are in general only well-defined on the universal covering of  $\Sigma$ .

**2.2. The associated family of flat connections.** The associated  $\mathbb{S}^1$ -family of minimal surfaces  $f_\lambda$  of a given minimal surface  $f: \Sigma \rightarrow \mathbb{S}^3$  can be complexified as follows: Identify  $\mathbb{S}^3 \cong \text{SU}(2)$  such that the round metric of curvature 1 is given by  $-\frac{1}{2} \text{tr}()$  on  $\mathfrak{su}(2) = T_e \text{SU}(2)$ . Decompose the Maurer-Cartan form

$$f^{-1}df = 2\Phi - 2\Phi^*$$

into its complex linear

$$\Phi \in \Omega^{(1,0)}(\Sigma, \mathfrak{su}(2) \otimes \mathbb{C}) = \Gamma(\Sigma, K_\Sigma \mathfrak{sl}(2, \mathbb{C}))$$

and its complex anti-linear

$$-\Phi^* \in \Omega^{(0,1)}(\Sigma, \mathfrak{su}(2) \otimes \mathbb{C}) = \Gamma(\Sigma, \bar{K}_\Sigma \mathfrak{sl}(2, \mathbb{C}))$$

parts, i.e.,

$$\Phi = \frac{1}{4}(f^{-1}df - i * f^{-1}df) \quad \text{and} \quad -\Phi^* = \frac{1}{4}(f^{-1}df + i * f^{-1}df).$$

Note that we use the convention  $*dz = idz$  and  $*d\bar{z} = -id\bar{z}$  for any local holomorphic coordinate on  $\Sigma$ .

Define

$$\nabla = d + \frac{1}{2}f^{-1}df = d + \Phi - \Phi^*$$

and

$$\nabla^\lambda := \nabla + \lambda^{-1}\Phi - \lambda\Phi^*.$$

By its very definition,  $\nabla^\lambda$  is unitary for all  $\lambda \in \mathbb{S}^1$ , and satisfies

$$\nabla^{\lambda=-1} = d \quad \text{and} \quad \nabla^{\lambda=1} = d + f^{-1}df = \nabla^{\lambda=-1}.f$$

i.e.,  $f$  is given as the gauge between  $\nabla^{\lambda=-1}$  and  $\nabla^{\lambda=1}$ . Since  $f$  is minimal and hence harmonic we have

$$d^\nabla * df = 0 \quad \iff \quad d^\nabla \Phi = 0.$$

A direct computation then shows that this is equivalent to flatness of  $\nabla^\lambda$  for all  $\lambda \in \mathbb{C}^*$ . Moreover, conformality of  $f$  is equivalent to

$$-\frac{1}{2} \text{tr}(\Phi^2) = 0$$

which (using  $\text{tr}(\Phi) = 0$  which holds by construction) is itself equivalent to  $\Phi$  being nilpotent. Zeros of  $\Phi$  are exactly the points where  $f$  is branched.

Conversely, given a family of flat  $\text{SL}(2, \mathbb{C})$  connections

$$(2.1) \quad \lambda \in \mathbb{C}^* \mapsto \nabla^\lambda = \nabla + \lambda^{-1}\Phi - \lambda\Phi^*$$

over the Riemann surface  $\Sigma$  satisfying

- $\nabla^\lambda$  is unitary for all  $\lambda \in \mathbb{S}^1 \subset \mathbb{C}^*$ ;
- $\nabla^{\lambda=\pm 1}$  are trivial;
- $\Phi \in \Gamma(\Sigma, K_\Sigma \mathfrak{sl}(2, \mathbb{C}))$  is a complex linear nilpotent nowhere vanishing 1-form;



then the gauge  $f$  satisfying

$$\nabla^1.f = \nabla^{-1}$$

is a conformal minimal immersion which is well-defined on  $\Sigma$ . For details see [17].

**2.3. The DPW approach.** The classical DPW approach [10] describes minimal surfaces in  $\mathbb{S}^3$  (and CMC surfaces in  $\mathbb{R}^3$ ) in terms of a holomorphic  $\mathfrak{sl}(2, \mathbb{C})$ -valued 1-form

$$\eta = \sum_{k \geq -1} \eta_k \lambda^k$$

on  $\Sigma$  depending meromorphically on a spectral parameter  $\lambda \in \mathbb{D}^* \subset \mathbb{C}^*$ . Here  $\mathbb{D}$  is a disc centered at  $\lambda = 0$  which contains the unit circle  $\mathbb{S}^1$ . The 1-form  $\eta$  is called a *DPW potential*.

The advantage of the DPW approach is that the potential  $\xi$  just needs to satisfy the conditions that its residue  $\text{res}_{\lambda=0} \eta = \eta_{-1}$  is nilpotent and nowhere vanishing. Then, the following procedure yields a minimal surface in  $\mathbb{S}^3$ : Consider a solution

$$d\Psi + \eta\Psi = 0$$

depending holomorphically (in  $\lambda$ ) on an initial condition  $\Psi(b)$ ,  $b \in \Sigma$  fixed. The map  $\Psi$  is called a *holomorphic frame*. Clearly,  $\Psi$  is only well-defined on the universal covering  $\tilde{\Sigma} \rightarrow \Sigma$  in general.

In a second step, consider the Iwasawa decomposition

$$\Psi = BF,$$

where

$$B: \tilde{\Sigma} \times \mathbb{D} \rightarrow \text{SL}(2, \mathbb{C})$$

is holomorphic on a disc  $\mathbb{D}$  of radius  $r > 1$  centered at 0, and

$$F: \tilde{\Sigma} \times \mathbb{D} \cap \mathbb{D}^{-1} \rightarrow \text{SL}(2, \mathbb{C})$$

is unitary (i.e.,  $\text{SU}(2)$ -valued) along  $\lambda \in \mathbb{S}^1 \subset \mathbb{D} \cap \mathbb{D}^{-1}$ . We call such maps  $B$  and  $F$  *positive* and *unitary loops*, respectively. The (loop group) Iwasawa decomposition always exists, and is unique if one normalizes  $B$  to be upper triangular with positive diagonal entries at  $\lambda = 0$  (see [28] or [10]).

Then,

$$(2.2) \quad \nabla^\lambda := (d + \eta).B = d.F^{-1}$$

is the associated family of flat connections of some minimal surface  $f: \tilde{\Sigma} \rightarrow \mathbb{S}^3$ , where  $d = d_{\tilde{\Sigma}}$  is the partial differential with respect to  $\tilde{\Sigma}$ . Note that the second equality follows from  $d\Psi + \eta\Psi = 0$  and  $\Psi = BF$ . Moreover, (2.2) directly implies that  $\nabla^\lambda$  is unitary for all  $\lambda \in \mathbb{S}^1$ , while  $\nabla^\lambda = (d + \eta).B$  then implies it is of the form (2.1) with nilpotent  $\lambda^{-1}$ -part  $\Phi = B(0)^{-1}\eta_{-1}B(0)$ .

The surface is well-defined on  $\Sigma$  provided the following two conditions are satisfied:

- (1)  $B$  is well-defined on  $\Sigma$ ;
- (2)  $d + \eta$  has trivial monodromy at  $\lambda = \pm 1$ .

In fact, (1) guarantees that  $\nabla^\lambda$  is well-defined on  $\Sigma$ , while  $d + \eta$  having trivial monodromy at  $\lambda = \pm 1$  then implies that the gauge equivalent connections  $\nabla^\lambda = (d + \eta).B$  has trivial monodromy at  $\lambda = \pm 1$  as well.

It should be noted here that there are no holomorphic DPW potentials that fulfill even only (1) on a compact Riemann surface of positive genus. In fact, the only holomorphic connection 1-form  $\eta \in H^0(\Sigma, K_\Sigma \mathfrak{sl}(2, \mathbb{C}))$  with unitary monodromy is given by  $\eta = 0$ . On the other hand, one can admit apparent singularities of  $\eta$  on  $\Sigma$  to fulfill (1) and (2).

In order to deal with condition (1), we first note that  $B$  being well-defined implies that  $d + \eta$  must have unitary monodromy (up to conjugation) for all  $\lambda \in \mathbb{S}^1$ . This necessary condition is in fact sufficient as well: if  $\Psi$  is a solution of  $d\Psi + \eta\Psi$  with unitary monodromy for all  $\lambda \in \mathbb{S}^1$

at  $b \in \Sigma$  for appropriate initial condition  $\Psi(b)$ , then one can deduce from the uniqueness of the Iwasawa decomposition that the positive term  $B$  in the factorization of the meromorphic frame  $\Psi = BF$  has trivial monodromy. Note that by an application of the Iwasawa decomposition theorem, the initial condition  $\Psi(b)$  can be chosen to be positive, i.e., to be a holomorphic map from  $\mathbb{D}$  to  $\mathrm{SL}(2, \mathbb{C})$ . Thus, by conjugating the potential with a positive initial condition  $\Psi(b)$ , we can always assume that the monodromy of the holomorphic (or rather meromorphic since we allow singularities on  $\Sigma$ ) frame  $\Psi$  at the base-point  $b$  with initial condition  $\Psi(b) = \mathbb{1}$  is actually unitary, provided the initial potential  $\eta$  has already unitary monodromy up to conjugation for all  $\lambda \in \mathbb{S}^1$ .

In order to construct compact minimal surfaces in  $\mathbb{S}^3$  we therefore seek for meromorphic DPW potentials  $\eta$  on  $\Sigma$  satisfying the following *closing conditions*:

- for any pole  $p$  of  $\eta$  on  $\Sigma$ , there is a positive gauge  $B$  such that  $(d+\eta).B$  extends smoothly through  $p$ ;
- the monodromy of  $d + \eta$  with respect to the base-point  $b \in \Sigma$  is unitary for all  $\lambda \in \mathbb{S}^1$  (*intrinsic closing condition*);
- the monodromy of  $d + \eta$  is trivial for  $\lambda = \pm 1$  (*extrinsic closing condition*).

**Remark 2.1.** In practice, it is often useful to rotate the spectral plane by some factor  $e^{i\varphi}$ . After doing that, the extrinsic closing condition is that the monodromy of  $d + \eta$  is trivial for  $\lambda_1 = e^{i\varphi}$  and  $\lambda_2 = -e^{i\varphi}$ , and the surface is obtained as the gauge between these two flat connections. We mainly use  $\lambda = \pm i$  as this is most natural for dealing with reflections, see e.g. Lemma 3.4 below or [1, Theorem 3.1].

The spectral parameters  $\lambda_1$  and  $\lambda_2 = -\lambda_1 \in \mathbb{S}^1$  for which  $\nabla^\lambda$  has trivial monodromy are called the *evaluation points* of the surface  $f$ . The minimal immersion  $f: \Sigma \rightarrow \mathbb{S}^3$  is then given by the explicit formula from [2]:

$$f = (F^{\lambda_1})^{-1} F^{\lambda_2}.$$

For a simply connected surface, the intrinsic and extrinsic closing conditions are vacuous, while on a compact Riemann surface of higher genus the conditions are very restrictive. Moreover, in the case of a compact Riemann surface of higher genus, the monodromy of  $\nabla^\lambda$  is irreducible for generic  $\lambda \in \mathbb{C}^*$ . The same also holds true for the potential  $d + \eta^\lambda$ . This observation implies that the choice of initial condition  $\Psi(b)$  is unique up to multiplication with a unitary loop  $F$  from the right. This multiplication does not change  $\nabla^\lambda$  in (2.2) and therefore produces the same minimal surface.

**Remark 2.2.** Dressing is a procedure which produces new minimal surfaces from existing one. In order to not change the topology of the immersion by a dressing transformation, it is necessary to have spectral parameters  $\lambda_0 \in \mathbb{C}^* \setminus \mathbb{S}^1$  at which  $\nabla^{\lambda_0}$  has abelian monodromy representation. As dressing (on higher genus surfaces) changes the conjugacy classes of the monodromy representations at finitely many spectral parameters, dressing changes the DPW potential  $\eta$  in a non-trivial way as well. Therefore, dressing transformations do not exist for the minimal surfaces considered in this paper as there are no additional abelian monodromies besides the trivial one for the evaluation points. It would be very interesting to have an example of a compact minimal (or CMC) surface of genus at least 2 which actually allows for non-trivial dressing transformations. For more details on dressing see for example [5] or [16] and the references therein.

**2.4. Reflection potentials.** Our aim is to construct and study compact minimal reflection surfaces  $f: \Sigma \rightarrow \mathbb{S}^3$ , i.e., reflection surfaces which are minimal. Examples of minimal reflection surfaces in  $\mathbb{S}^3$  built from fundamental quadrilaterals in fundamental tetrahedra include the following:

- the minimal Lawson surfaces [26];
- and minimal surfaces constructed by Karcher-Pinkall-Sterling [22].

By definition, the fundamental region  $P$  of a minimal reflection surface is a topological disc. We can therefore apply results from [1] about the existence of DPW potentials. If the number of vertices of  $P$  is even, it is shown in [1, Proposition 5.5] that there is a meromorphic DPW potential  $\xi$  on  $\mathbb{CP}^1$  generating  $f$  in the following way: the order 2 subgroup  $\Gamma < G$  of orientation preserving symmetries acts on  $\Sigma$  by holomorphic automorphisms, and the quotient Riemann surface is given by  $\pi: \Sigma \rightarrow \Sigma/\Gamma = \mathbb{CP}^1$ . Then  $\eta = \pi^*\xi$  is a meromorphic DPW potential on  $\Sigma$  satisfying the above three closing conditions. Furthermore, in the case of the Lawson surfaces  $\xi_{1,g}$  with  $n = 4$  vertices, it is shown in [11] that the DPW potential  $\xi$  is actually Fuchsian, i.e., of the form

$$\xi = \sum_{k=1}^4 A_k \frac{dz}{z - p_k}$$

for some  $A_k: \mathbb{D}^* \rightarrow \mathfrak{sl}(2, \mathbb{C})$  constant in  $z$ . We expect, without having a general proof, that all minimal reflection surfaces can be constructed by Fuchsian DPW potentials, which motivates the following definition.

**Definition 2.3.** A *reflection potential* is a Fuchsian DPW potential on  $\mathbb{CP}^1$

$$(2.3) \quad \xi = \sum_{k=1}^p \frac{A_k}{z - z_k} dz$$

with  $p$  simple poles  $z_1, \dots, z_p \in \mathbb{S}^1$  (and no pole at  $\infty$ ) satisfying the following conditions:

- The potential satisfies the reality condition

$$(2.4) \quad \overline{\tau^* \xi(\bar{\lambda})} = \xi(\lambda) \quad \text{for } \tau(z) := 1/\bar{z} \text{ ,}$$

- The eigenvalues of each  $A_k$  are  $\lambda$ -independent and contained in the interval  $(-\frac{1}{2}, \frac{1}{2})$ .

The ( $\lambda$ -independent) eigenvalues  $\pm\nu_k$  of  $A_k$  encode the dihedral angle  $\theta$  of the adjacent reflection planes at  $z_k$  of a minimal reflection surface. In fact, we have

$$(2.5) \quad \theta = \begin{cases} 2\pi\nu_k & \text{if } \nu_k \in (0, \frac{1}{4}] \\ \pi - 2\pi\nu_k & \text{if } \nu_k \in (\frac{1}{4}, \frac{1}{2}) \end{cases} .$$

Relationship (2.5) follows from [1, Theorem 3.3] since the monodromy along a simple closed curve around  $z_k$  is conjugated to  $\exp(2\pi i A_k)$ . By [1, Theorem 3.5] the eigenvalues of the residues  $A_k$  have to be  $\pm\frac{1}{2n_k}$  or  $\pm\frac{n_k-1}{2n_k}$  in order for  $f$  being immersed at  $z_k$  (or rather at its preimages in  $\Sigma$ ). For later use, we call the first and the second case of (2.5) to be of *spin* -1 and of *spin* 1, respectively. See [1] for more details about the spin of a potential, and its relationship with the spin structure of an immersion.

We choose a base-point  $b \in \mathbb{S}^1 \subset \mathbb{CP}^1$ . The monodromy of the meromorphic frame  $\Psi$  for a reflection potential  $\xi$  is computed with initial condition  $\Psi(b) = \mathbb{1}$ .

Let  $\mathbb{S}^1 \subset \mathbb{CP}^1$  be divided into  $p$  segments  $s_1, \dots, s_p$  at  $p$  distinct consecutive points  $z_k$ ,  $k = 1, \dots, p$ , dividing  $s_k$  and  $s_{k+1}$  (or  $s_p$  and  $s_1$ ). Let  $\xi$  be a reflection potential on  $\mathbb{CP}^1$  with singularities at these points  $z_k$ . With  $b$  a base-point on  $\mathbb{S}^1$ , for  $i, j \in \{1, \dots, n\}$  let  $\gamma_{ij}$  be a simple closed counterclockwise curve based at  $b$  which crosses the segments  $s_i$  and  $s_j$ , and let  $M_{ij}$ ,  $i, j \in \{1, \dots, n\}$ ,  $i < j$  be the monodromy of a meromorphic frame  $\Psi$  for  $\xi$  along  $\gamma_{ij}$ . The  $n$  *local* monodromies are those along paths which enclose one singularity; the remaining monodromies are called *global*.

We then have the following theorem.

**Theorem 2.4.** [1, Theorem 3.3] *If the meromorphic frame  $\Psi$  of a reflection potential  $\xi$*

- *has unitary monodromy on  $\mathbb{S}^1$ , and*

- its local and global logarithmic monodromy eigenvalues are correct, i.e., at the evaluation points  $\lambda_l$ ,  $l = 1, 2$ , we have

$$(2.6) \quad \frac{1}{2} \operatorname{tr} M_{ij}|_{\lambda_l} = \pm \cos \theta_{ij}, \quad i, j \in \{1, \dots, n\}, \quad i < j,$$

then the unit disk maps to a minimal polygon whose boundaries reflect in  $p$  totally geodesic spheres  $P_1, \dots, P_p$ , with internal dihedral angles  $\theta_{i,j}$  between  $P_i$  and  $P_j$ .

In (2.6), the appropriate sign on the right hand side can be determined by using the spin of a potential. For details, see [1, Section 3.4]. In the case at hand of a reflection surface, the angles are of the form  $\theta_{ij} = \frac{\pi}{n}$ , where  $n \in \mathbb{N}^{\geq 2}$  is the vertex integer of the corresponding point, compare with Definition 1.6.

**2.5. The flow.** Finding reflection potentials satisfying the closing conditions is a difficult task, as this requires a detailed understanding of the monodromy representations of Fuchsian systems. At the moment, no reflection potential of a reflection surface of genus  $g \geq 2$  is known explicitly. On the other hand, the existence of the Lawson surfaces  $\xi_{g,1}$  has been proven recently by showing the existence of reflection potentials satisfying the closing conditions via an implicit function theorem argument, at least for genus large enough, see [14] and also [12, 15]. In [14], the positive eigenvalue of the residue  $A_1$  (or equivalently  $A_l$  for any  $l = 1, \dots, 4$ ) has been used as a flow parameter. One can then reformulate the implicit function theorem as a flow. This flow has

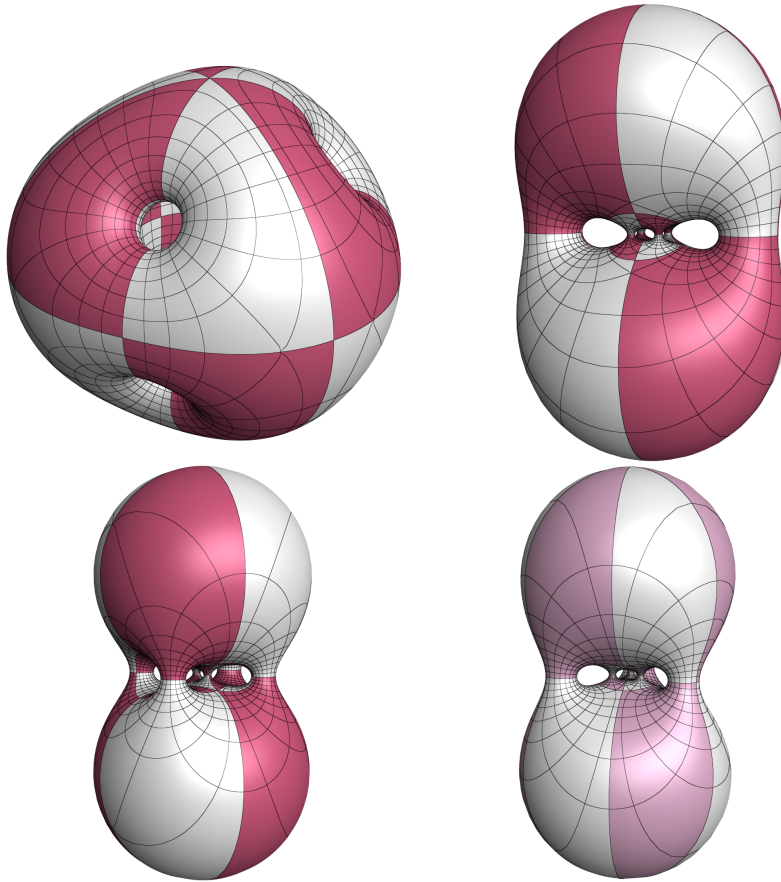


FIGURE 7. Four views (stereographic projections) of the surface  $B_{3,2}$  of genus 5.

been numerically implemented and extended to other surface classes with reflection potentials with 4 vertices, see [1]. In the following, we report on our numerical experiments with reflection potentials with more than 4 vertices.

Given  $F : \mathbb{R} \times \mathbb{R}^n \rightarrow \mathbb{R}^n$ , then  $x : \mathbb{R} \rightarrow \mathbb{R}^n$  satisfying  $F(t, x) = 0$  can be computed by solving the differential equation

$$(2.7) \quad \frac{dF}{dt} + \frac{dF}{dx} \frac{dx}{dt} = 0 .$$

The free variables  $x$  for the flow are:

- the poles of the potential, and
- the coefficients of the residues of the potential as a finite approximated Laurent series.

As such, these variables encode the geometric parameters:

- the conformal type of the surface in terms of the poles,
- the local and global logarithmic monodromy eigenvalues, and
- the mean curvature  $H$  via the evaluation points  $\lambda_1 \neq \lambda_2 \in \mathbb{S}^1$  (with  $\lambda_2 = -\lambda_1$  for minimal surfaces).

The flow runs over the interval  $t \in [0, 1]$ .

The constraints  $F$  for the flow are

- sum condition:  $\sum_{k=1}^p A_k = 0$ .
- determinant condition: the  $\lambda^{-1}$  coefficient  $\xi^{(-1)}$  of  $\xi$  has determinant zero and is nowhere vanishing.
- eigenvalue condition: the eigenvalues of  $A_k$  are constant in  $\lambda$  and specified, see (2.5).
- intrinsic closing constraints: the monodromy representation is contained in  $SU_2$  (at appropriately many sample points) along  $\mathbb{S}^1$ ,
- extrinsic closing constraints: the monodromy at the evaluation points is specified, see (2.6).

The geometric parameters are chosen appropriately according to the target surface, as follows. For flows through minimal surfaces in  $\mathbb{S}^3$ ,

- The conformal type is left free by fixing three of the poles and leaving the others free on  $\mathbb{S}^1$ .
- the local and global logarithmic monodromy eigenvalues are set to be linear functions of  $t$  so as to have the desired target values at  $t = 1$ .
- The evaluation points are fixed to  $\lambda = \pm i$ .

Other flows are possible with other choices of constraints on the geometric parameters. For example, to flow through CMC surfaces instantiating a fixed reflection surface (fixed local and global logarithmic monodromy eigenvalues), the conformal type is made to depend on  $t$  and the evaluation points  $\lambda_1, \lambda_2 \in \mathbb{S}^1$  are left free.

For the case of the Lawson surfaces  $\xi_{g,1}$ , the above finite dimensional flow approximates the infinite-dimensional flow constructed in [14]. Using the theory of parabolic Deligne-Hitchin moduli spaces (see e.g. [13] and the references therein), reflection potentials satisfying the closing conditions can be interpreted as holomorphic sections of the Deligne-Hitchin moduli spaces satisfying a reality constraint. A native dimension count then suggest that the experimental flow (2.7) can be set up to model deformations of reflection potentials satisfying the closing conditions. With that, our experiments suggest that these deformations are in fact generically possible and unique as long as the parameters are carefully chosen, e.g., fixing the monodromy at the evaluation points and the mean curvature  $H$  to be contained in a given reflection group should determine the conformal type locally.

### 3. Lawson surface potentials

In this section we discuss the existence of reflection potentials for the Lawson surfaces with arbitrarily many poles  $p$ . These potentials serve as initial conditions for numerical experiments. In particular, for the case  $p = 5$ , Theorem 3.5 constructs

- a 5-pole potential for the Lawson surface  $\xi_{1,2}$  with a fundamental polygon bounded by three planes, and
- a 5-pole potential for the Lawson surface  $\xi_{1,3}$  with a fundamental polygon bounded by four planes.

These are used as the initial potentials for flows to all the surfaces constructed from fundamental pentagons. Both these potentials are seen numerically to extend holomorphically to the punctured unit  $\lambda$  disk.

Fuchsian DPW potentials for Lawson surfaces with 5 or more poles are computed in Theorem 3.5 by a combination of pushdowns, pullbacks, gauges and coordinate changes, starting from the 4-pole Fuchsian DPW potential for Lawson surface constructed in [14, 11]. The following technical lemmas are required to compute these potentials.

A *flip gauge*  $g$  of a Fuchsian potential  $\xi$  is a gauge transformation  $g$  (possibly only well-defined up to  $g \mapsto -g$ ) such that  $\xi.g = g^{-1}dg + g^{-1}\xi g$  is again Fuchsian and such that the pole set of  $\xi.g$  is either the same as or is a subset of the pole set of  $\xi$ .

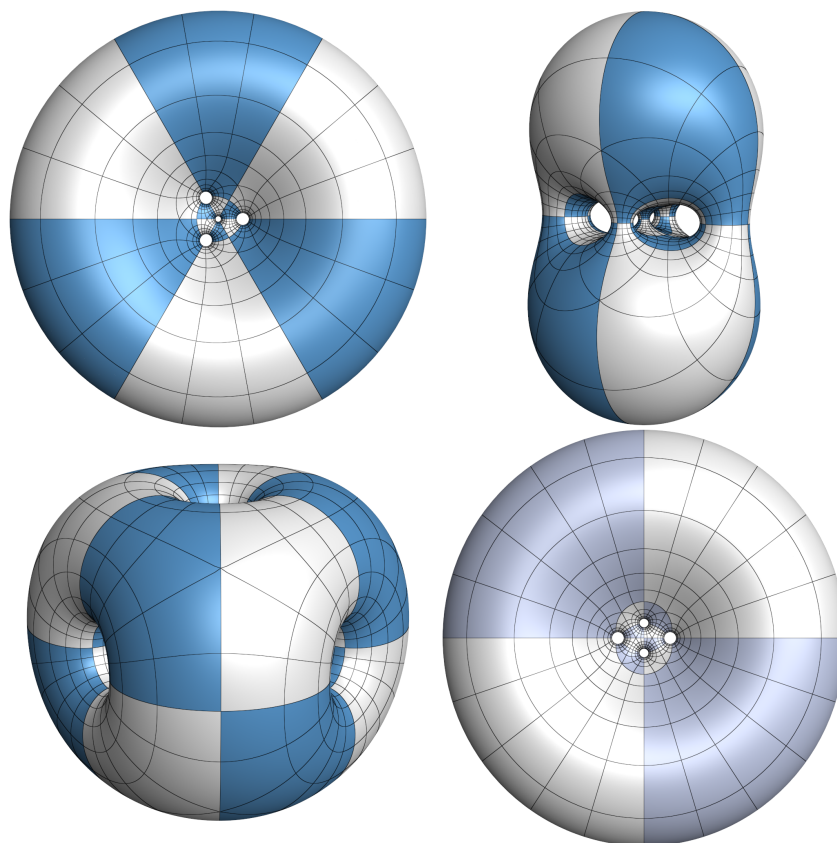


FIGURE 8. Four views (stereographic projections) of surface  $B_{2,3}$  of genus 4.

In the following, an *eigenline* of a residue  $R$  of a Fuchsian potential is a holomorphic map from a neighborhood of  $\lambda = 0$  to  $\mathbb{C}^2 \setminus (0, 0)^\top$  which is an eigenline of  $R$ .

**Lemma 3.1.** *Let  $\xi$  be a Fuchsian DPW potential with simple poles at  $z = p$  and  $z = \infty$  and respective residues  $A$  and  $B$  with eigenvalue in  $\mathbb{R}^*$ . Let  $\ell$  and  $m$  be the eigenlines of  $A$  and  $B$  with respect to their respective positive eigenvalues. Let  $h = (\ell, m)$  be the  $2 \times 2$  matrix valued map with columns  $\ell$  and  $m$ . If  $\det h$  is nonzero at  $\lambda = 0$ , then with*

$$(3.1) \quad g := hk \quad , \quad k := \text{diag}((z-p)^{-1/2}, (z-p)^{1/2})$$

is a flip gauge for  $\xi$ .

Moreover, if the positive eigenvalue of  $A$  is  $1/2$  and the monodromy around  $p$  is  $-\mathbb{1}$ , then  $\xi.g$  does not have a pole at  $0$ .

*Proof.* Compute that  $h^{-1}Ah$  is upper triangular and  $h^{-1}Bh$  is lower triangular. Then gauging  $\xi$  by  $g$  does not add any poles to  $\xi$ , so  $g$  is a flip gauge for  $\xi$ .

The last statement follows since  $\xi.g$  has monodromy  $\mathbb{1}$  around  $p$  and its residue at  $p$  has eigenvalues  $0$ . Hence, the residue vanishes as claimed.  $\square$

In principle, applying a flip gauge can produce apparent singularities of the potential inside the unit spectral disc. This happens exactly when the eigenlines  $\ell$  and  $m$  fall together.

**Lemma 3.2.** *Consider*

$$\tau(z) := -z \quad , \quad \sigma = \text{diag}(i, -i)$$

and let  $\xi$  be a Fuchsian DPW potential with symmetry

$$(3.2) \quad \tau^* \xi := \xi . \sigma \quad .$$

Then there exists a Fuchsian DPW potential  $\eta$  such that

$$(3.3) \quad \xi.g = f^* \eta \quad , \quad g := \text{diag}(z^{1/2}, z^{-1/2}) \quad , \quad f(z) := z^2 \quad .$$

*Proof.* The potential  $\xi.g$  is invariant under  $\tau$ , so it is the pull back of a potential  $\eta$  under  $f$ .  $\square$

**Lemma 3.3.** *Let*

$$(3.4) \quad \xi = \frac{A}{z-p} dz + \frac{B}{z-\tau(p)} dz + \frac{C}{z-q} dz + \frac{D}{z-\tau(q)} dz$$

be a 4-pole Fuchsian DPW potential on  $\mathbb{C}P^1$ , where  $\tau$  is an involutive Möbius transform. If

- $\det A = \det B$
- $\det C = \det D$
- the kernels of  $A^{(-1)}$  and  $B^{(-1)}$  (the  $\lambda^{-1}$  coefficients of  $A$  and  $B$ ) are independent

then there exists a  $z$ -independent gauge  $g$  such that  $\eta := \xi.g$  satisfies the symmetry

$$(3.5) \quad \tau^* \eta = \eta . \sigma \quad , \quad \sigma := \text{diag}(i, -i) \quad .$$

*Proof.* The last condition implies that

$$(3.6) \quad h := \frac{A+B}{\sqrt{\det(A+B)}} = -\frac{C+D}{\sqrt{\det(C+D)}}$$

is holomorphic at  $\lambda = 0$ . From the first and second condition we obtain by using  $\text{tr} A = 0 = \text{tr} B = \text{tr} C = \text{tr} D$  that  $Ah = hB$  and  $Ch = hD$ .

Since  $\text{tr} h = 0$ , there exists  $g$  holomorphic at  $\lambda = 0$  such that  $h = g\sigma g^{-1}$ . Namely,  $g = (m_1, m_2)$ , where the columns  $m_1$  and  $m_2$  are the independent eigenlines of  $h$  corresponding to the eigenvalues  $\pm i$ .

From  $B = h^{-1}Ah$  and  $D = h^{-1}Ch$  we observe

$$(3.7) \quad g^{-1}Bg = \sigma^{-1}(g^{-1}Ag)\sigma \quad \text{and} \quad g^{-1}Dg = \sigma^{-1}(g^{-1}Cg)\sigma .$$

Hence  $\eta := \xi.g = g^{-1}\xi g$  has the required symmetry (3.5).  $\square$

**Lemma 3.4.** *Let  $\xi$  be a Fuchsian potential with poles on  $\mathbb{S}^1$  with unitarizable generically irreducible monodromy. Assume that  $\xi$  induces a minimal surface  $f$  in  $\mathbb{S}^3$  which reflects across each arc of  $\mathbb{S}^1$  for the evaluation points  $\lambda_{1/2} = \pm i$ . Then there exists a  $z$ -independent gauge  $g$  such that  $\eta = \xi.g$  satisfies the symmetry (3.2). Moreover, for every  $b \in \mathbb{S}^1$  distinct from the poles of  $\xi$ , we can chose a  $z$ -independent gauge  $g = g_b$  such that  $\eta = \xi.g$  has unitary monodromy with respect to the base-point  $b$ .*

*Proof.* As  $\xi$  has unitarizable monodromy, we can assume without loss of generality that  $\xi$  already has unitary monodromy with respect to the base-point  $b \in \mathbb{S}^1$ . Therefore, the minimal surface  $f$  is obtained by the following process

- solve  $d\Psi + \xi\Psi = 0$  with  $\Psi(b) = \mathbb{1}$ ;
- factor  $\Psi = BF$  into positive part  $B$  and unitary part  $F$ ;
- then  $f = (F^{\lambda=-i})^{-1}F^{\lambda=i}$  (up to possible spherical isometries).

We claim that

$$d + \tau^*\overline{\eta(\bar{\lambda})}$$

with the same initial condition  $\Psi(b) = \mathbb{1}$  yields the reflected surface of  $f$ . In fact  $\tau^*\overline{\Psi(\bar{\lambda})}$  solves

$$(d + \tau^*\overline{\eta(\bar{\lambda})})\tau^*\overline{\Psi(\bar{\lambda})} = 0$$

with  $\tau^*\overline{\Psi(\bar{\lambda})}(b) = \mathbb{1}$ . Then we have the Iwasawa factorization

$$\tau^*\overline{\Psi(\bar{\lambda})} = \tau^*\overline{B(\bar{\lambda})}\tau^*\overline{F(\bar{\lambda})}$$

into positive and unitary part, so that we obtain in the third step the reflected surface

$$\tilde{f} = \tau^*\overline{F(\bar{\lambda} = -i)}^{-1}\tau^*\overline{F(\bar{\lambda} = i)} = \tau^*\tilde{f}^{-1} = \tau^*f^t$$

as claimed.

Consider the positive gauge  $g_1$  satisfying

$$(d + \eta(\lambda)).g_1 = d + \alpha_\lambda$$

for the associated family of flat connections, with  $g_1(b) = \mathbb{1}$ . This gauge is obtained as  $g_1 = B$  in the factorisation  $\Psi = BF$  where  $\Psi$  solves  $d\Psi + \xi\Psi = 0$  with  $\Psi(b) = \mathbb{1}$ .

By assumption  $f$  satisfies  $\tau^*f = f^t$ , so that there exists a positive gauge  $g_2$  with

$$(d + \tau^*\overline{\eta(\bar{\lambda})}).g_2 = d + \alpha_\lambda.$$

We have  $g_2(b) = \mathbb{1}$  as well.

Then,  $g = g_1g_2^{-1}$  is a positive gauge satisfying

$$d + \tau^*\overline{\eta(\bar{\lambda})} = (d + \eta(\lambda)).g$$

and

$$g(b) = \mathbb{1}.$$

We claim that  $g$  is constant in  $z$ . In fact, any gauge between two Fuchsian systems can be singular only at points where the eigenvalues of the residues of the two Fuchsian systems differ by half-integers. But  $d + \tau^*\overline{\eta(\bar{\lambda})}$  and  $d + \eta(\lambda)$  have the same eigenvalues (2.5), so singularities of  $g$  can only occur at points with eigenvalues of the residues being  $\pm\frac{1}{4}$ . To prove that this is not possible either, we just observe that such a singular gauge  $g$  would change the  $\lambda^{-1}$ -behaviour at the corresponding residue: if the  $\lambda^{-1}$ -part of the residue does not vanish before applying the



singular gauge  $g$  (the spin -1 case in the framework of [1]) it does vanish afterwards (the spin 1 case), and vice versa. This is not possible, as  $d + \tau^* \overline{\eta(\lambda)}$  and  $d + \eta(\lambda)$  have the same spin at all corresponding singular points. As  $\mathbb{CP}^1$  is compact and  $g$  is holomorphic,  $g$  is constant in  $z$ . As  $g(b) = \text{Id}$  this proves the statement.  $\square$

**Theorem 3.5.** (1) For each  $n \in \mathbb{N}_{\geq 2}$ , there exists a reflection potential for the Lawson surface  $\xi_{1, n-1}$  with  $n+2$  poles on  $\mathbb{S}^1$ , each with positive residue eigenvalue  $1/4$ . The unit disk is the domain for a minimal  $(n+2)$ -gon in  $\mathbb{S}^3$  whose boundary lies in a polytope bounded by 3 planes.

(2) For each even  $n \in \mathbb{N}_{\geq 2}$ , there exists a reflection potential for the Lawson surface  $\xi_{1, n-1}$  with  $n/2 + 3$  poles on  $\mathbb{S}^1$ , each with positive residue eigenvalue  $1/4$ . The unit disk is the domain for a minimal  $(n/2 + 3)$ -gon in  $\mathbb{S}^3$  whose boundary lies in a polytope bounded by 4 planes.

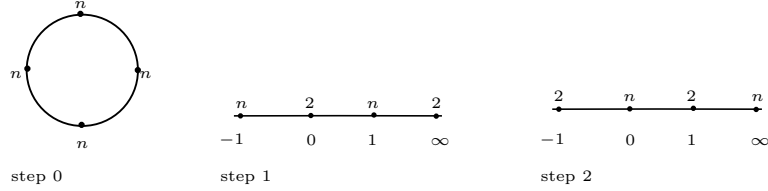
*Proof.* We first show the following: For each  $n \in \mathbb{N}_{\geq 2}$  there exists a Fuchsian DPW potential  $\xi$  for the Lawson surface  $\xi_{1, n-1}$  with 4 poles at  $(-1, 0, 1, \infty)$  with respective vertex integers  $(2, n, 2, n)$  and the symmetry

$$(3.8) \quad \tau^* \xi = \xi \cdot \sigma, \quad \tau(z) = -1/z, \quad \sigma = \text{diag}(i, -i).$$

(Recall that the vertex integers  $n$  are linked to the eigenvalues by (2.5) and  $\theta = \frac{\pi}{n}$ . By abuse of notation, we therefore call  $n$  the vertex integer of the corresponding singularity of the reflection potential.)

Step 0. By [11], the Lawson surface  $\xi_{1, n-1}$  has a 4-pole Fuchsian DPW potential  $\xi$  with poles at  $(1, i, -1, -i)$ , spin  $-1$  at each pole, and respective vertex integers  $(n, n, n, n)$  satisfying the symmetry

$$(3.9) \quad \tau^* \xi := \xi \cdot \sigma, \quad \tau(z) := -z, \quad \sigma = \text{diag}(i, -i).$$



Step 1. Push down by  $z \mapsto z^2$  via Lemma 3.2. The resulting potential has four simple poles at  $(-1, 0, 1, \infty)$  with respective vertex integers  $(n, 2, n, 2)$ .

Step 2. Apply the coordinate change taking  $(-1, 0, 1, \infty) \rightarrow (0, 1, \infty, -1)$ . The resulting potential has four simple poles at  $(-1, 0, 1, \infty)$  with respective vertex integers  $(2, n, 2, n)$ .

Step 3. Apply the symmetrizing gauge (Lemma 3.3) so that the resulting potential has the same poles and vertex integers, and satisfies the symmetry (3.8).

To show the existence of this symmetrizing gauge, note that the residues of the potential obtained in step 2 are

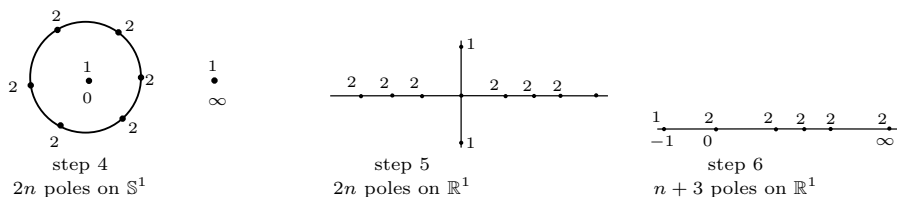
$$(3.10) \quad A_{-1} = \begin{bmatrix} \frac{1}{4} & -a_0 + ia_1 \\ 0 & -\frac{1}{4} \end{bmatrix}, \quad A_0 = \begin{bmatrix} b_0 & a_0 \\ c_0 & -b_0 \end{bmatrix}, \quad A_1 = \begin{bmatrix} -\frac{1}{4} & 0 \\ -c_0 - ic_1 & \frac{1}{4} \end{bmatrix}, \quad A_\infty = \begin{bmatrix} b_1 & -ia_1 \\ c_1 & -b_1 \end{bmatrix}.$$

Since the Hopf differential for a Lawson surface  $\xi_{1, n}$ ,  $n > 0$ , is not 0, the real quantities  $a_0^{(-1)}$  and  $a_1^{(-1)}$  are not both zero, and the real quantities  $c_0^{(-1)}$  and  $c_1^{(-1)}$  are not both zero. Hence  $(-a_0 + ia_1)^{(-1)} \neq 0$  and  $(-c_0 - ic_1)^{(-1)} \neq 0$ . Hence the kernels of  $A_{-1}^{(-1)}$  and  $A_1^{(-1)}$  are respectively  $(1, 0)^\top$  and  $(0, 1)^\top$ , which are independent. Hence the symmetrizing gauge exists by Lemma 3.3.

**Lawson potentials with a fundamental polygon bounded by three planes.** We claim that for each  $n \in \mathbb{N}_{\geq 2}$ , there exists a reflection potential for the Lawson surface  $\xi_{1, n-1}$  with  $n+2$  poles on  $\mathbb{S}^1$ , each with positive residue eigenvalue  $1/4$ . The unit disk is the domain for a minimal  $(n+2)$ -gon in  $\mathbb{S}^3$  whose boundary lies in a polytope bounded by 3 planes.

Start with the potential constructed in step 3 above.

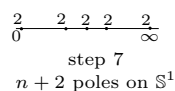
Step 4. Pull back by  $z \mapsto z^n$ . With  $\alpha := e^{i\pi/n}$ , the resulting potential has  $2n$  simple poles at the  $(2n)$ th roots of unity  $\{\alpha^k \mid k \in \{0, \dots, 2n-1\}\}$  each with vertex integer 2, and poles at 0 and  $\infty$  with vertex integer 1.



Step 5. Apply the coordinate change taking  $\mathbb{S}^1$  to  $\mathbb{R}$ ,  $\alpha^{1/2} \rightarrow 0$  and  $-\alpha^{1/2} \rightarrow \infty$ . The resulting potential has  $2n$  simple poles on  $\mathbb{R}$  each with vertex integer 2, and poles at  $i$  and  $-i$  with vertex integer 1. This potential has the symmetry

$$(3.11) \quad \tau^* \xi = \xi \cdot \sigma, \quad \sigma(z) := -z, \quad \sigma := \text{diag}(i, -i).$$

Step 6. Push down by  $z \mapsto z^2$ . The resulting potential has  $n+2$  simple poles on  $\mathbb{R}^{>0}$ , each with vertex integer 2, a simple pole  $\infty$  with integer 2 and a simple pole at  $-1$  with vertex integer 1.



Step 7. Remove the pole at  $-1$  by a flip gauge as in Lemma 3.1. The resulting potential has  $n+2$  poles on  $\mathbb{R}^1$ .

To check the existence of the gauge, since all residues have spin  $-1$ , let  $k_r$  be the kernels of the  $-1$  coefficients of the residues. Since the Lawson surface does not have zero Hopf differential, then the  $k_r$  are not all dependent. Hence the kernel of the  $-1$  coefficient of the residue at  $-1$  is independent of the kernel of the  $-1$  coefficient of the residue at another pole. Hence the gauge exists by Lemma 3.1.

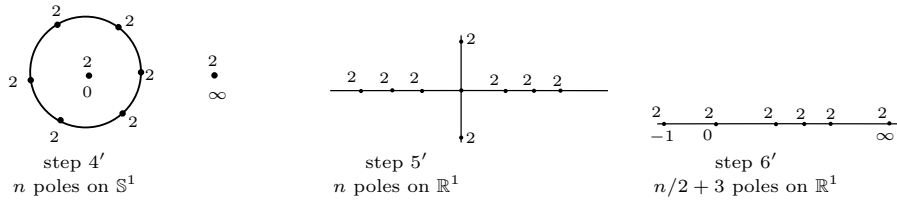
Step 8. Apply a coordinate change mapping  $\mathbb{R} \rightarrow \mathbb{S}^1$ . The resulting potential has  $n+2$  simple poles on  $\mathbb{S}^1$ , each with vertex integer 2.

Step 9. Apply a  $z$ -independent gauge as in Lemma 3.4, so that the potential has the real symmetry (2.4).

**Lawson potentials with a fundamental polygon bounded by four planes.** We now prove the following: For each even  $n \in \mathbb{N}_{\geq 2}$ , there exists a reflection potential for the Lawson surface  $\xi_{1, n-1}$  with  $n/2+3$  poles on  $\mathbb{S}^1$ , each with positive residue eigenvalue  $1/4$ . The unit disk is the domain for a minimal  $(n/2+3)$ -gon in  $\mathbb{S}^3$  whose boundary lies in a polytope bounded by 4 planes.

Start with the potential constructed in step 3 above.

Step 4'. Pull back by  $z \mapsto z^{n/2}$ . The resulting potential has  $n+2$  simple poles:  $n$  on  $\mathbb{S}^1$  at the  $n$ th roots of unity  $\{\beta^k \mid k \in \{1, \dots, n-1\}\}$ ,  $\beta := e^{2\pi i/n}$ , and poles at 0 and  $\infty$ . Each pole has vertex integer 2.



Step 5'. Apply the coordinate change taking  $\mathbb{S}^1 \rightarrow \mathbb{R}$ ,  $\alpha^{1/2} \rightarrow 1$  and  $-\alpha^{1/2} \rightarrow i$  and  $-i$ . The resulting potential has  $2n + 2$  poles:  $n$  poles on  $\mathbb{R}$ , and two poles at  $\pm i$ , each with vertex integer 2. This potential has the symmetry

$$(3.12) \quad \tau^* \xi = \xi \cdot \sigma, \quad \sigma(z) := -z, \quad \sigma := \text{diag}(i, -i).$$

Step 6'. Push down by  $z \mapsto z^2$ . The resulting potential has  $n/2 + 3$  simple poles on  $\mathbb{R}$ , each with vertex integer 2.

Step 7'. Apply a coordinate change taking  $\mathbb{R} \rightarrow \mathbb{S}^1$ . The resulting potential has  $n/2 + 3$  simple poles on  $\mathbb{S}^1$ , each with vertex integer 2.

Step 8'. Apply a  $z$ -independent gauge as in Lemma 3.4 so that the potential has the symmetry (2.4).  $\square$

#### 4. Area

The flow of the DPW potential affords a numerical calculation of the area of the reflection surfaces. For doing so, we apply Corollary 4.3 of [15] for the situation at hand. Before stating and proving the area formula for a minimal reflection surface in terms of the entries of its reflection potential, we first recall some notations and make some simple observations.

Let

$$(4.1) \quad \xi = \sum_k R_k \frac{dz}{z - z_k}$$

be a reflection potential for a minimal reflection surface  $f: \Sigma \rightarrow \mathbb{S}^3$ . As all poles of  $\xi$  are on the unit circle, the residue condition  $\sum_k R_k = 0$  must hold. Let  $G$  be the corresponding reflection group. Note that its order  $|G|$  is finite since  $\Sigma$  is compact by definition of a reflection surface in  $\mathbb{S}^3$ .

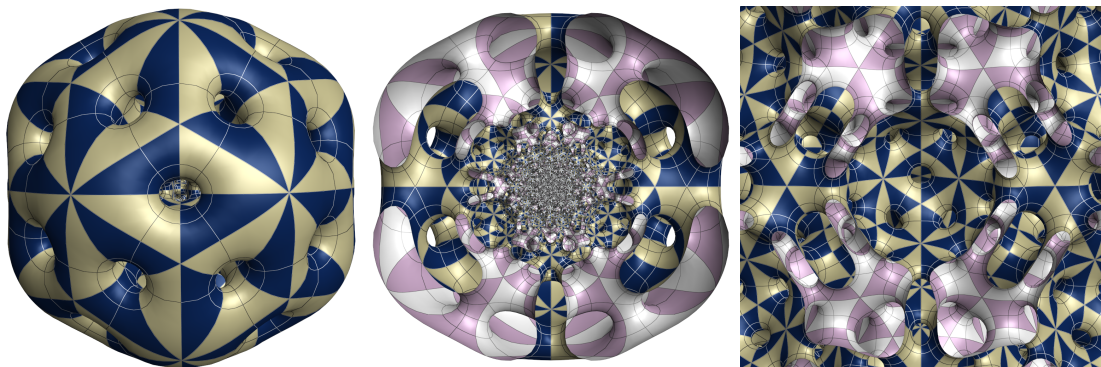


FIGURE 9. The non-dihedral reflection surface with the highest genus 5161. The surface has the symmetry of the 600-cell of order 14400. Left to right: the full surface, a cutaway showing half the surface, and a closeup of the center of the cutaway.

Let  $\Gamma \subset G$  be the subgroup of index 2 consisting of orientation preserving maps. Then  $\Gamma$  acts on  $\Sigma$  by holomorphic automorphisms, and we obtain the following lemma.

**Lemma 4.1.** *There is a holomorphic map  $\pi: \Sigma \rightarrow \Sigma/\Gamma = \mathbb{CP}^1$  which branches exactly over the preimages of  $z_1, \dots, z_p$ . The preimage of the open unit disc consists of  $|G|$  many copies of the fundamental polygon  $P$ .*

Let  $p \in \Sigma$  be a branch point, i.e., the preimage of a branch value  $\pi(p) = z_k$ . Then its branch order  $b_p$  satisfies

$$(4.2) \quad b_p = n_k - 1 ,$$

where  $n_k$  the vertex integer of the point  $z_k$ .

For  $k = 1, \dots, p$  define

$$(4.3) \quad m_k := \frac{|\Gamma|}{n_k} = \frac{|G|}{2n_k} .$$

Obviously,  $m_k \in \mathbb{N}^{>0}$  is the number of preimages of  $z_k$  of  $\pi: \Sigma \rightarrow \mathbb{CP}^1$ .

Recall that the eigenvalues of the residue  $R_k$  of  $\xi$  at  $z_k$  are

$$(4.4) \quad \begin{cases} \pm \frac{1}{2n_k} & \text{if } \xi \text{ has spin } -1 \text{ at } z_k \\ \pm \frac{n_k-1}{2n_k} & \text{if } \xi \text{ has spin } 1 \text{ at } z_k \end{cases} ,$$

independently of  $\lambda$ .

If  $z_k$  has spin 1, then

$$(4.5) \quad \operatorname{res}_{\lambda=0} R_k = 0$$

by section 2.4 in [1].

If  $z_k$  has spin  $-1$ ,

$$(4.6) \quad \operatorname{res}_{\lambda=0} R_k \neq 0$$

as  $f$  is an immersion (see Section 2.4 in [1]). Since the eigenvalues of  $R_k$  are independent of  $\lambda$ ,  $R_k$  is nilpotent. Consequently, there is a matrix  $C_k \in \mathrm{SL}_2\mathbb{C}$  such that

$$(4.7) \quad C_k^{-1} R_k C_k = \frac{1}{2n_k} \begin{bmatrix} a & b/\lambda \\ c\lambda & -a \end{bmatrix}$$

for holomorphic functions  $a, b, c: \mathbb{D}_{1+\epsilon} \rightarrow \mathbb{C}$ . Here,  $\mathbb{D}_{1+\epsilon}$  is the disc of radius  $1 + \epsilon > 1$  centered at  $\lambda = 0$  in the spectral plane, for which the reflection potential is defined. Then,

$$(4.8) \quad \alpha_k := \frac{a(0)}{2n_k} \in \mathbb{C}$$

is independent of the choice of  $C_k$  (amongst all  $C_k$  satisfying (4.7) for some holomorphic functions  $a, b, c$ ), and is called the *area defect* of  $\xi$  at the spin  $-1$  point  $z_k$ .

With these notations we have the following theorem.

**Theorem 4.2.** *Let  $\xi = \sum_k R_k \frac{dz}{z-z_k}$  be a reflection potential for the minimal reflection surface  $f: \Sigma \rightarrow \mathbb{S}^3$  with finite order reflection group  $G$ . Let  $n_k$  be vertex integer of  $z_k$  and  $m_k$  be the number of preimages of  $z_k$  in  $\Sigma$ . Assume that  $\xi$  has spin  $-1$  at  $z_1, \dots, z_r$ , and spin  $1$  at  $z_{r+1}, \dots, z_p$ . Let  $\alpha_k$  be the area defect at  $z_k$  for  $k = 1, \dots, r$ . Then, the area of  $f$  is given by*

$$(4.9) \quad A(f) = 2\pi \sum_{k=1}^r (1 - 2n_k \alpha_k) m_k .$$

*Proof.* To prove the area formula, we will make use of Corollary 4.3 of [15]. The surface is obtained globally from the pull-back potential  $\pi^*\xi$ . In order to apply [15] we have to find at any singular point  $p$  of  $\pi^*\eta$  a local gauge transformation  $G^p$  which depends holomorphically on  $\lambda$  such that

$$(4.10) \quad (d - \pi^*\xi).G_p$$

is smooth at  $p$ . It turns out to be easier to work on a twofold covering  $\hat{\pi}: \hat{\Sigma} \rightarrow \Sigma$  which branches exactly over  $\pi^{-1}(\{z_1, \dots, z_p\})$ . Such a covering exists.

First, let  $k \in \{1, \dots, r\}$ , i.e.,  $\eta$  has spin -1 at  $z_k$ . Write  $C_k^{-1}R_kC_k = \frac{1}{2n_k} \begin{bmatrix} a & b/\lambda \\ c\lambda & -a \end{bmatrix}$  for holomorphic functions  $a, b, c$  defined on an open neighborhood of  $\lambda = 0$  after a  $\lambda$ -independent conjugation  $C_k \in \text{SL}_2\mathbb{C}$ . Since the eigenvalues of  $R_k$  at the spin -1 point  $z_k$  are  $\pm \frac{1}{2n_k}$ , it holds

$$(4.11) \quad -a^2 - bc = -1 .$$

Consider a local holomorphic coordinate  $z$  centered at  $z_k$ . As  $\pi$  is branched over  $z_k$  with branch order  $n_k - 1$  and  $\hat{\pi}$  is a two fold covering which singly branches over every  $\pi^{-1}(z_k)$ , there is local holomorphic coordinate  $y$  on  $\hat{\Sigma}$  centered at  $\hat{p} := \hat{\pi}^{-1}(p)$  satisfying

$$(4.12) \quad y = z^{2n_k} .$$

Take the pull-back  $\mu = (\hat{\pi} \circ \pi)^*\xi$  of the potential  $\xi$  on  $\hat{\Sigma}$ . It expands at a preimage  $y_k = (\pi \circ \hat{\pi})^{-1}(z_k)$  as

$$(4.13) \quad \mu = \begin{bmatrix} a & b/\lambda \\ c\lambda & -a \end{bmatrix} \frac{dy}{y} + y^2(\dots)$$

since  $n_k > 1$  by assumption. Consider the local gauge

$$(4.14) \quad G^p = C_k \begin{bmatrix} \kappa & 0 \\ \lambda & \kappa^{-1} \end{bmatrix} \begin{bmatrix} y^{-1} & 0 \\ 0 & y \end{bmatrix}$$

where  $\kappa$  is defined by

$$(4.15) \quad \kappa = \frac{b}{1-a} .$$

Note that  $\kappa$  is holomorphic and non-vanishing at  $\lambda = 0$  if  $a(0) \neq 1$ , which we assume first.

Then,

$$(4.16) \quad (d - \mu).G^p = \begin{bmatrix} 0 & 0 \\ \frac{b\lambda(a^2+bc-1)}{(a-1)^2} & 0 \end{bmatrix} \frac{dy}{y^3} + y^0(\dots)$$

is holomorphic at  $y_k \in \hat{\Sigma}$  since  $a^2 + bc = 1$ . Expanding  $G^p = G_0^p + G_1^p\lambda + \dots$  in terms of  $\lambda$  gives

$$(4.17) \quad G_0^p = \begin{bmatrix} -\frac{b_0}{(a_0-1)z} & 0 \\ 0 & -\frac{(a_0-1)z}{b_0} \end{bmatrix}$$

and

$$(4.18) \quad G_1^p = \begin{bmatrix} \frac{-a_0b_1+a_1b_0+b_1}{(a_0-1)^2z} & 0 \\ \frac{1}{z} & -\frac{z(-a_0b_1+a_1b_0+b_1)}{b_0^2} \end{bmatrix}$$

where  $a = a_0 + a_1\lambda + \dots$ ,  $b = b_0 + b_1\lambda + \dots$ . Note that

$$(4.19) \quad a(0) = a_0 = 2n_k\alpha_k .$$

We obtain

$$(4.20) \quad \text{res}_{\hat{p}} \text{tr}(\mu_{-1}G_1^k(G_0^k)^{-1}) = (1 - a_0) = (1 - 2n_k\alpha_k) ,$$

where  $\mu = \mu_{-1}\lambda^{-1} + \mu_0 + \dots$ .

If  $a(0) = 1$ , there is a positive (and constant in  $y$ ) conjugator  $H^1$  (there are several cases to consider depending on  $a$  and  $b$ , but the result is always the same) such that

$$(4.21) \quad (H^1)^{-1} \begin{bmatrix} a & b/\lambda \\ c\lambda & -a \end{bmatrix} H^1 = \begin{bmatrix} 1 & * \\ 0 & -1 \end{bmatrix}.$$

In particular, the pole can be removed by gauging with  $G^k := H^1 H^2$  where  $H^2 = \begin{bmatrix} y^{-1} & 0 \\ 0 & y \end{bmatrix}$ , and a direct computation shows that we obtain

$$(4.22) \quad \operatorname{res}_{\hat{p}} \operatorname{tr}(\mu_{-1} G_1^k (G_0^k)^{-1}) = 0 = (1 - a_0) = (1 - 2n_k \alpha_k).$$

At points  $z_k$  where  $\eta$  has spin 1, i.e.,  $k > r$ , we know from Section 2.4 in [1] that  $R_k$  has vanishing  $\lambda^{-1}$ -term. In particular, we find a positive conjugator  $H^1$  such that

$$(4.23) \quad (H^1)^{-1} R_k H^1 = \begin{bmatrix} n_k - 1 & 0 \\ 0 & 1 - n_k \end{bmatrix},$$

so that  $G^k = H^1 H^2$  with

$$(4.24) \quad H^2 = \begin{bmatrix} y^{1-n_k} & 0 \\ 0 & y^{n_k-1} \end{bmatrix}$$

is a gauge which desingularizes  $\mu$  at  $\pi^{-1}(p)$ . Then, a short computation shows

$$(4.25) \quad \operatorname{res}_{\hat{p}} \operatorname{tr}(\mu_{-1} G_1^k (G_0^k)^{-1}) = 0.$$

Note that there are exactly  $|G|/(2n_k) = m_k$  many preimages of  $z_k$  on  $\hat{\Sigma}$ . The immersion  $f \circ \hat{\pi}: \hat{\Sigma} \rightarrow \mathbb{S}^3$  has twice the area as  $f$ , and we therefore obtain from Corollary 4.3 of [15]

$$(4.26) \quad A(f) = 2\pi \sum_{k=1}^r (1 - 2n_k \alpha_k) m_k$$

as claimed. □

Applying the area formula, we obtain numerical values for the areas of experimentally constructed reflection surfaces. We list these values below for some of the surfaces. We like to emphasize that our numerical values for the Lawson surfaces agree well with the values of other experiments by very different methods, e.g., using Brakke's surface evolver [18]. Even more convincing, however, is the high agreement between our experimentally determined area of Lawson surfaces and the area values of [6] with proven error estimates: for  $g \geq 5$  the error estimate in [6] is  $\leq 10^{-5}$ . On the other hand, the values determined in [6] and the numerical values from Table (8) also differ at most by  $\leq 10^{-5}$ .

Finally, it is shown in [25] that the area of the Lawson surfaces  $\xi_{k,k}$  have limiting behaviour

$$A(\xi_{k,k}) \sim 8\pi(1 - \frac{1}{\sqrt{2}})k + O(1),$$

which was actually first predicted from looking at Table (8).

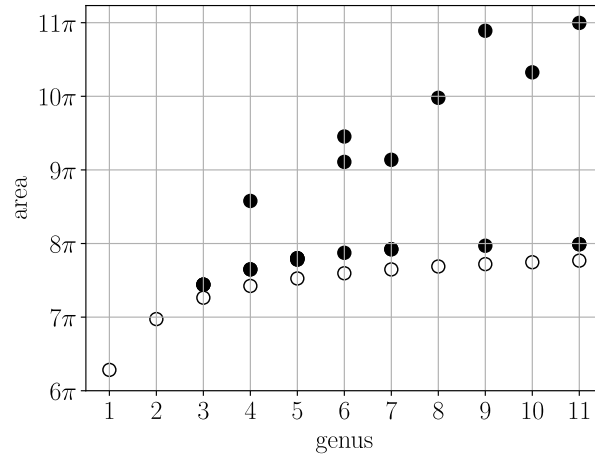


TABLE 7. This graph shows the area of embedded minimum surfaces of low genus examples of types  $A_{k,\ell}$  and  $B_{k,\ell}$ . The conjectured minimal areas are indicated by circles.

Area of  $A_{k,\ell}$ :

	2	3	4	5	6	7	8	9	10	11	12	13
2	19.7392	21.9085	22.8203	23.3219	23.6413	23.8635	24.0273	24.1532	24.2532	24.3345	24.4020	24.4588
3		26.9496	29.7001	31.3506	32.4381	33.2068	33.7788	34.2210	34.5731	34.8603	35.0990	35.3005
4			34.2138	37.2281	39.3296	40.8618	42.0230	42.9314	43.6607	44.2586	44.7575	45.1802
5				41.5084	44.6718	47.0665	48.9264	50.4055	51.6066	52.5996	53.4335	54.1431
6					48.8213	52.0800	54.6783	56.7842	58.5182	59.9666	61.1924	62.2420
7						56.1460	59.4707	62.2178	64.5135	66.4534	68.1098	69.5381
8							63.4786	66.8516	69.7121	72.1579	74.2663	76.0984
9								70.8168	74.2267	77.1762	79.7434	81.9919
10									78.1591	81.5980	84.6193	87.2865
11										85.5045	88.9669	92.0471
12											92.8523	96.3341
13												100.202

TABLE 8. Area of the  $A_{k,\ell}$  surfaces.

Area of  $B_{k,\ell}$ :

	1	2	3	4	5
2	21.9085	22.8203	24.0331	24.5041	24.7364
3	23.3787	24.4459	28.7061		
4	24.0262	24.8879			
5	24.4518	25.0380			

TABLE 9. Area of the  $B_{k,\ell}$  surfaces.

### References

1. A. Bobenko, S. Heller, and N. Schmitt, *Constant mean curvature surfaces based on fundamental quadrilaterals*, Math. Phys. Anal. Geom. **24** (2021), no. 4, Paper No. 37, 46.
2. A.I. Bobenko, *Constant mean curvature surfaces and integrable equations*, Uspekhi Mat. Nauk **46** (1991), no. 4, 3–42.

3. A.I. Bobenko, T. Hoffmann, and N. Smeenk, *Constant mean curvature surfaces from ring patterns: Geometry from combinatorics*, in preparation, 2024.
4. A.I. Bobenko, T. Hoffmann, and B. Springborn, *Minimal surfaces from circle patterns: Geometry from combinatorics*, *Annals of Mathematics* **164** (2006), no. 1, 231–264.
5. F. E. Burstall, J. F. Dorfmeister, K. Leschke, and A. C. Quintino, *Darboux transforms and simple factor dressing of constant mean curvature surfaces*, *Manuscripta Math.*, vol 140, 1-2, 2013, pp. 213–236.
6. S. Charlton, L. Heller, S. Heller, and M. Traizet, *Minimal surfaces and alternating multiple zetas*, in preparation, 2024.
7. H. S. M. Coxeter, *Discrete groups generated by reflections.*, *Ann. Math. (2)* **35**, 1934, pp. 588–621.
8. H. S. M. Coxeter, *The complete enumeration of finite groups of the form  $R_i^2 = (R_i R_j)^{k_{ij}} = 1$* , *Journal of the London Mathematical Society* (1935), no. 1, 21–25.
9. M. Davis, *The geometry and topology of Coxeter groups*, Somerville, MA: International Press; Beijing: Higher Education Press, 2015, pp. 129–142.
10. J. Dorfmeister, F. Pedit, and H. Wu, *Weierstrass type representation of harmonic maps into symmetric spaces*, *Comm. Anal. Geom.* **6** (1998), no. 4, 633–668.
11. L. Heller and S. Heller, *Fuchsian DPW potentials for Lawson surfaces*, *Geom. Dedicata* **217** (2023), no. 6, Paper No. 101, 32.
12. L. Heller, S. Heller, and N. Schmitt, *Navigating the space of symmetric CMC surfaces*, *J. Differ. Geom.* **110**, 2018, pp. 413–455.
13. L. Heller, S. Heller, and M. Traizet, *Loop group methods for the non-abelian hodge correspondence on a 4-punctured sphere*, arxiv:2205.12106.
14. ———, *Complete families of embedded high genus cmc surfaces in the 3-sphere*, arXiv:2108.10214, 2021.
15. L. Heller, S. Heller, and M. Traizet, *Area estimates for high genus Lawson surfaces via DPW*, *J. Differential Geom.* **124** (2023), no. 1, 1–35.
16. S. Heller, *A spectral curve approach to lawson symmetric cmc surfaces of genus 2*, *Math. Ann.* **360**, no.3-4, 607–652, 2014.
17. N. J. Hitchin, *Harmonic maps from a 2-torus to the 3-sphere*, *J. Differential Geom.* **31**, no.3, 627–710, 1990.
18. L. Hsu, R. Kusner, and J. Sullivan, *Minimizing the squared mean curvature integral for surfaces in space forms*, *Experimental Mathematics* **3**, 1992, pp. 191–207.
19. N. Kapouleas, *Minimal surfaces in the round three-sphere by doubling the equatorial two-sphere, I*, *J. Differential Geom.* **106** (2017), no. 3, 393–449.
20. N. Kapouleas and P. McGrath, *Minimal surfaces in the round three-sphere by doubling the equatorial two-sphere, II*, *Comm. Pure Appl. Math.* **72** (2019), no. 10, 2121–2195.
21. N. Kapouleas and D. Wiygul, *The Lawson surfaces are determined by their symmetries and topology*, *J. Reine Angew. Math.* **786**, 2022, pp. 155–173.
22. H. Karcher, U. Pinkall, and I. Sterling, *New minimal surfaces in  $S^3$* , *J. Differential Geom.* **28** (1988), no. 2, 169–185.
23. M. Karpukhin, R. Kusner, P. McGrath, and D. Stern, *Embedded minimal surfaces in  $S^3$  and  $B^3$  via equivariant eigenvalue optimization*, arxiv:2402.13121, 2024.
24. D. Ketover, *Equivariant min-max theory*, 2016.
25. M. Traizet L. Heller, S. Heller, *Lawson  $\xi_{k,k}$  surfaces*, in preparation, 2024.
26. H. Lawson, Jr., *Complete minimal surfaces in  $S^3$* , *Ann. of Math. (2)* **92** (1970), 335–374.
27. F. Marques and A. Neves, *Min-max theory and the Willmore conjecture*, *Ann. Math. (2)* **179**, 2014, pp. 683–782.
28. Andrew Pressley and Graeme Segal, *Loop groups*, Oxford Math. Monogr., 1986.

INSTITUT FÜR MATHEMATIK, TU BERLIN, STR. DES 17. JUNI 136, 10623 BERLIN, GERMANY  
 Email address: bobenko@math.tu-berlin.de

BEIJING INSTITUTE OF MATHEMATICAL SCIENCES AND APPLICATIONS, BEIJING, CHINA  
 Email address: sheller@bimsa.cn

INSTITUT FÜR MATHEMATIK, TU BERLIN, STR. DES 17. JUNI 136, 10623 BERLIN, GERMANY  
 Email address: schmitt@math.tu-berlin.de